Placenta 35 (2014) 848–851

Contents lists available at ScienceDirect

Placenta

journal homepage: www.elsevier.com/locate/placenta

Short communication

Circulating levels of maternal plasma cell-free pregnancy-associated placenta-specific microRNAs are associated with placental weight

K. Miura [a, *], S. Morisaki [a], S. Abe [a], A. Higashijima [a], Y. Hasegawa [a], S. Miura [a], S. Tateishi [a], H. Mishima [b], K. Yoshiura [b], H. Masuzaki [a]

[a] Department of Obstetrics and Gynecology, Nagasaki University Graduate School of Biomedical Sciences, 1-7-1 Sakamoto, Nagasaki 852-8501, Japan
[b] Department of Human Genetics, Nagasaki University Graduate School of Biomedical Sciences, Nagasaki, Japan

ARTICLE INFO

Article history:
Accepted 6 June 2014

Keywords:
Placenta-specific microRNA
Maternal plasma
Circulating level
Placental weight

ABSTRACT

The aim of this study was to investigate the relationship between plasma concentration of cell-free pregnancy-associated placenta-specific microRNAs and clinical variables (placental weight, maternal body mass index, and neonatal birth weight). Circulating levels of cell-free pregnancy-associated placenta-specific microRNAs (miR-515-3p, miR-517a, miR-517c and miR-518b) in maternal plasma were measured by quantitative real-time RT-PCR in sixty-two pregnant women. The levels of cell-free pregnancy-associated placenta-specific microRNAs were significantly associated with placental weight, but not associated with body mass index or birth weight. Therefore, the measurement of cell-free pregnancy-associated placenta-specific miRNAs levels in maternal plasma may reflect the pregnancy status related to placenta volume.

© 2014 Elsevier Ltd. All rights reserved.

1. Introduction

Recently, we have identified pregnancy-associated placenta-specific miRNAs (miR-515-3p, miR-517a, miR-517c, miR-518b and miR-526b), which locate on chromosome 19 miRNA cluster (C19MC) region, in the plasma of pregnant women [1,2]. To date, several placental miRNAs are involved in, or associated with, pregnancy-associated disorders, such as preeclampsia, fetal growth restriction or preterm delivery and, therefore, have a strong potential for use as sensitive and specific biomarkers [3–5]. A major source of cell-free placental miRNAs in maternal plasma is the villous trophoblast, which is able to release exosomes containing miRNAs into the maternal circulation [6,7], suggesting their potential for becoming novel biomarkers for prediction and detection of pathologies in pregnancy. Although the placenta is a source of supply for cell-free pregnancy-associated placenta-specific miRNAs (cfpp-miRNAs) [1,2], which factors affect the plasma concentration of cfpp-miRNA remain unknown.

Here, to increase knowledge of factors affecting the circulating levels of cfpp-miRNAs in maternal plasma, we investigated its association with placental weight (PW) as the placental factor, maternal body mass index (BMI) as the maternal factor and neonatal birth weight (BW) as the fetal factor. Also, as the pregnancy-associated but not placenta-specific miRNA [2], we measured the plasma concentration of cell-free miR-323-3p, and investigated its association with PW, BMI and BW.

2. Materials and methods

2.1. Sample collection

All samples were obtained after receiving written informed consent, and the Institutional Review Board of Nagasaki University approved the study protocol.

Women with smoking, multiple gestations, placenta previa, or invasive placentation, preterm labor, infection, fetal anomalies or aneuploidy, fetal growth restriction, or preeclampsia were excluded. Finally, we obtained maternal blood from 62 women with uncomplicated pregnancies of a singleton at 37–38 weeks to exclude the possibility of preterm labor. Gestational age was assessed using ultrasonography. All women had nothing to eat or drink for 8 h prior to blood collection. Maternal blood samples (7 mL) were collected within 3 h of elective cesarean section (CS) delivery. At the time of blood sampling, they had no signs of labor. Preparation and extraction of total RNA containing small RNA molecules were performed as described previously [2,8].

2.2. Real-time qRT-PCR analysis of miRNAs

All specific primers and TaqMan probes (miR-515-3p, miR-517a, miR-517c, miR-518b and miR-323-3p) were purchased from TaqMan MicroRNA Assays (Applied Biosystems, Warrington, UK). Absolute quantitative real-time RT-PCR (qRT-PCR) of miRNAs in plasma samples was performed as described previously [1,2,8,9]. For each miRNA assay, we prepared a calibration curve by 10-fold serial dilution of single-stranded cDNA oligonucleotides corresponding to each miRNA sequence from 1.0×10^2 to 1.0×10^8 copies/mL. Each sample and each calibration dilution was analyzed in triplicate. Each assay could detect down to 100 RNA copies/mL [2,8,9].

* Corresponding author. Tel.: +81 95 819 7363; fax: +81 95 819 7365.
E-mail address: kiyonori@nagasaki-u.ac.jp (K. Miura).

http://dx.doi.org/10.1016/j.placenta.2014.06.002
0143-4004/© 2014 Elsevier Ltd. All rights reserved.

Every batch of amplifications included three water blanks as negative controls for each of the reverse transcription and PCR steps. All data were collected and analyzed using a LightCycler® 480 Real-Time PCR System (Roche, Pleasanton, CA, USA).

2.3. Statistical analysis

Pearson product-moment correlation coefficients between plasma concentration of cfpp-miRNAs and clinical variables (PW, BMI or BW) were analyzed with SPSS version 19 (IBM Japan, Tokyo, Japan). Significances were defined as $P < 0.05$. To eliminate spurious correlation between circulating levels of cfpp-miRNAs and PW, BMI or BW, a partial correction coefficient analysis was performed.

3. Results and discussion

Median (minimum–maximum) levels of cfpp-miRNAs in maternal plasma were 5395.11 (1528.15–72734.98) copies/mL for miR-515-3p, 36338.12 (1789.61–909253.60) copies/mL for miR-517a, 29708.01 (1327.62–457445.24) copies/mL for miR-517c and 8492.21 (211.9–528026.51) copies/mL for miR-518b (Fig. 1a–d). As pregnancy-associated but not placenta-specific miRNA, median (minimum–maximum) levels of miR-323-3p in maternal plasma were 148131.34 (7669.99–2990112.52) copies/mL. Median (minimum–maximum) of PW, BMI, and BW were 573 (390–900) g, 20.2 (16.2–36.6), and 2995 (2274–3972) g, respectively. No relationship was detected between PW and BMI (r and *P*-value: 0.161 and 0.212). While, a significant association was seen between PW and BW, and between BMI and BW (*r* and *P*-values: 0.592 and <0.01, and 0.287 and <0.05, respectively).

The plasma concentrations of cfpp-miRNAs are associated with PW, but not associated with BMI or BW (Table 1, Fig. 1a–d). Previous reports support our data that PW affects the plasma concentrations of cfpp-miRNAs. Syncytiotrophoblast microparticles (STBM) and exosomes including fetal/placental DNAs/RNAs are released into maternal circulation of normal third trimester pregnancies, and their numbers are significantly higher in preeclampsia [10]. Their circulating levels may reflect the rate of syncytiotrophoblast apoptosis [11]. The placental factors, e.g. STBM and exosomes, in maternal blood damage the maternal endothelium, and then cause a syndrome of systemic endothelial dysfunction [12], indicating that increased concentration of STBM and exosomes is associated with the pathogenesis of preeclampsia [13–15]. Multiple pregnancy, which seems to have a larger volume of placenta in comparison to uncomplicated singleton pregnancy, is known to be one of the risk factors of preeclampsia [16,17]. Further, increased plasma concentration of cell-free placental miRNAs on C19MC region has been reported in preeclampsia [3]. Therefore, it seems to be reasonable that PW as a placental factor affects the plasma concentration of cfpp-miRNAs. Our previous study also

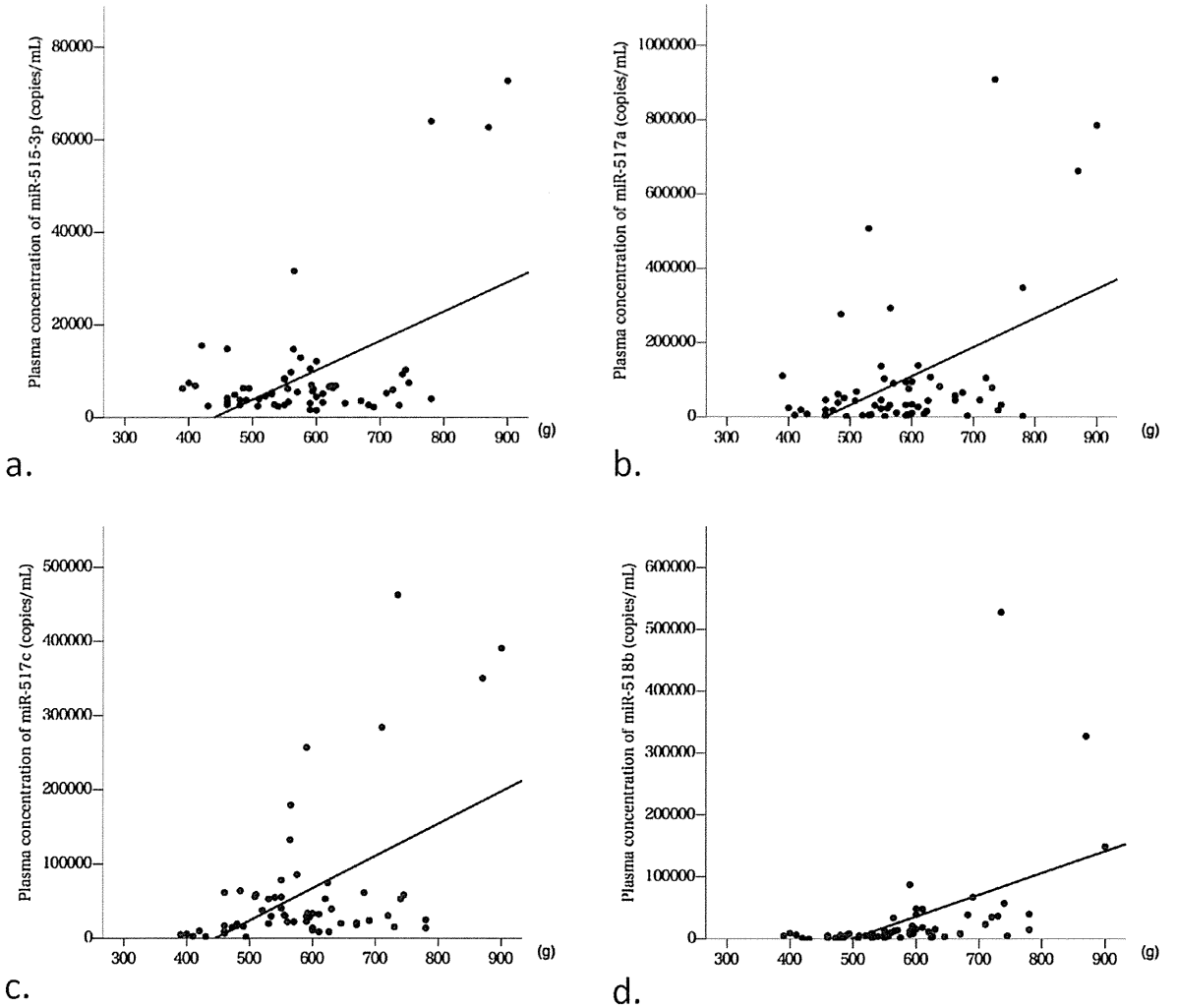

Fig. 1. Graph showing relationship between plasma concentration of cell-free pregnancy-associated placenta-specific miRNAs and placental weight. The correlation coefficient between placental weight and cell-free pregnancy-associated placenta-specific miRNAs levels for a. miR-515-3p is 0.506 (*P*-value: <0.01), for b. miR-517a is 0.475 (*P*-value: <0.01), for c. miR-517c is 0.512 (*P*-value: <0.01) and for d. miR-518b is 0.489 (*P*-value: <0.01).

Table 1
The summary of correlation coefficient analysis between plasma concentrations of cell-free pregnancy-associated miRNAs and clinical variables.

Pregnancy-associated miRNAs	Expression pattern	Statistical analysis	Clinical variables					
			Placental weight[a]		Maternal body mass index[a]		Neonatal birth weight[b]	
			r-value	*P*-value	*r*-value	*P*-value	*r*-value	*P*-value
miR-515-3p	Placenta-specific expression	Pearson product-moment correlation coefficient	0.506	<0.01	0.048	0.710	0.237	0.64
		Partial correction coefficient	0.467	<0.001	−0.021	0.870	−0.083	0.527
miR-517a	Placenta-specific expression	Pearson product-moment correlation coefficient	0.475	<0.01	−0.01	0.991	0.228	0.075
		Partial correction coefficient	0.434	<0.001	−0.072	0.583	−0.056	0.669
miR-517c	Placenta-specific expression	Pearson product-moment correlation coefficient	0.512	<0.01	0.117	0.366	0.225	0.079
		Partial correction coefficient	0.482	<0.001	0.056	0.668	−0.127	0.334
miR-518b	Placenta-specific expression	Pearson product-moment correlation coefficient	0.489	<0.01	−0.006	0.965	0.275	0.03
		Partial correction coefficient	0.420	0.001	−0.092	0.480	0.004	0.976
miR-323-3p	Embryonic and placental expression	Pearson product-moment correlation coefficient	0.066	0.678	−0.180	0.254	0.086	0.59
		Partial correction coefficient	0.007	0.965	−0.224	0.159	0.132	0.417

Significances were defined as *P*-value<0.05. To eliminate spurious correlation between plasma concentrations of cell-free pregnancy-associated miRNAs and placental weight, *maternal body mass index or neonatal birth weight, a partial correction coefficient analysis was performed.*

[a] The data of neonatal birth weight was used as controlled variable.

[b] The data of placental weight and maternal body mass index were used as controlled variables.

identified the miR-323-3p as pregnancy-associated miRNA in maternal plasma [2]. However, the expression pattern of miR-323-3p, which locates on chromosome 14 miRNA cluster region (C14MC), is expressed in embryonic and placental tissues, and in adult, it is restricted to brain [4]. Therefore, as pregnancy-associated but not placenta-specific miRNA in maternal plasma, plasma concentration of cell-free miR-323-3p was analyzed to clarify its association with clinical variables (PW, BMI or BW). We confirmed that plasma concentration of miR-323-3p is not associated with PW, BMI or BW (Table 1).

This is the first study to investigate the association between the circulating plasma concentration of cfpp-miRNAs and clinical variables (PW, BMI and BW). Here, we found that increased PW is associated with higher circulating levels of cfpp-miRNAs in plasma of pregnant woman. Alterations to placental miRNA expression have been associated with in utero exposures [18,19], and pregnancy-associated disease [20,21]. Therefore, the measurement of cfpp-miRNAs levels in maternal plasma may reflect the pregnancy status related to placenta volume, and provide important information on the pathogenesis of pregnancy-associated diseases, though it is necessary that more elaborate studies (more specimens, more mechanistic details) confirm our results. To clarify the biological mechanism and clinical application of circulating cfpp-miRNAs, other clinical factors that influence the circulating levels of these molecules in maternal plasma remain an area for future investigation.

Author contributions

All authors confirm that they have contributed to the intellectual content of this paper and have met the following requirements: (1) significant contributions to the conception and design, acquisition of data, or analysis and interpretation of data; (2) drafting or revising the article for intellectual content; and (3) final approval of the published article.

Grant/funding support

K.M., S.M. and H.M. were supported by JSPS KAKENHI, by grant numbers 26462495, 24791712, and 22591827, respectively.

Conflict of interest

None of the authors have any conflict of interest.

Acknowledgments

We would like to thank Dr. Akira Kinoshita for technical assistance.

References

[1] Chiu RW, Lo YM. Pregnancy-associated microRNAs in maternal plasma: a channel for fetal-maternal communication? Clin Chem 2010;56:1656–7.
[2] Miura K, Miura S, Yamasaki K, Higashijima A, Kinoshita A, Yoshiura K, et al. Identification of pregnancy-associated microRNAs in maternal plasma. Clin Chem 2010;56:1767–71.
[3] Hromadnikova I, Kotlabova K, Ondrackova M, Kestlerova A, Novotna V, Hympanova L, et al. Circulating C19MC microRNAs in preeclampsia, gestational hypertension, and fetal growth restriction. Mediators Inflamm 2013;2013:186041.
[4] Morales-Prieto DM, Ospina-Prieto S, Chaiwangyen W, Schoenleben M, Markert UR. Pregnancy-associated miRNA-clusters. J Reprod Immunol 2013;97:51–61.
[5] Zhao Z, Moley KH, Gronowski AM. Diagnostic potential for miRNAs as biomarkers for pregnancy-specific diseases. Clin Biochem 2013;46:953–60.
[6] Donker RB, Mouillet JF, Chu T, Hubel CA, Stolz DB, Morelli AE, et al. The expression profile of C19MC microRNAs in primary human trophoblast cells and exosomes. Mol Hum Reprod 2012;18:417–24.
[7] Luo SS, Ishibashi O, Ishikawa G, Ishikawa T, Katayama A, Mishima T, et al. Human villous trophoblasts express and secrete placenta-specific microRNAs into maternal circulation via exosomes. Biol Reprod 2009;81:717–29.
[8] Higashijima A, Miura K, Mishima H, Kinoshita A, Jo O, Abe S, et al. Characterization of placenta-specific microRNAs in fetal growth restriction pregnancy. Prenat Diagn 2013;33:214–22.
[9] Hasegawa Y, Miura K, Furuya K, Yoshiura KI, Masuzaki H. Identification of complete hydatidiform mole pregnancy-associated microRNAs in plasma. Clin Chem 2013;59:1410–2.
[10] Knight M, Redman CW, Linton EA, Sargent IL. Shedding of syncytiotrophoblast microvilli into the maternal circulation in pre-eclamptic pregnancies. Br J Obstet Gynaecol 1998;105:632–40.
[11] Sargent IL, Germain SJ, Sacks GP, Kumar S, Redman CW. Trophoblast deportation and the maternal inflammatory response in pre-eclampsia. J Reprod Immunol 2003;59:153–60.
[12] Cockell AP, Learmont JG, Smárason AK, Redman CW, Sargent IL, Poston L. Human placental syncytiotrophoblast microvillous membranes impair maternal vascular endothelial function. Br J Obstet Gynaecol 1997;104:235–40.
[13] *Redman CW, Sargent IL. Placental debris, oxidative stress and pre-eclampsia.* Placenta 2000;21:597–602.
[14] Redman CW, Sargent IL. Circulating microparticles in normal pregnancy and pre-eclampsia. Placenta 2008;29:S73–7.
[15] Redman CW, Tannetta DS, Dragovic RA, Gardiner C, Southcombe JH, Collett GP, et al. Review: does size matter? Placental debris and the pathophysiology of pre-eclampsia. Placenta 2012;33:S48–54.
[16] Duckitt K, Harrington D. Risk factors for pre-eclampsia at antenatal booking: systematic review of controlled studies. Br Med J 2005;330:565.
[17] Redman CW, Sargent IL. Latest advances in understanding preeclampsia. Science 2005;308:1592–4.

[18] Avissar-Whiting M, Veiga KR, Uhl KM, Maccani MA, Gagne LA, Moen EL, et al. Bisphenol A exposure leads to specific microRNA alterations in placental cells. Reprod Toxicol 2010;29:401–6.
[19] Maccani MA, Avissar-Whiting M, Banister CE, McGonnigal B, Padbury JF, Marsit CJ. Maternal cigarette smoking during pregnancy is associated with downregulation of miR-16, miR-21, and miR-146a in the placenta. Epigenetics 2010;5:583–9.
[20] Pineles BL, Romero R, Montenegro D, Tarca AL, Han YM, Kim YM, et al. Distinct subsets of microRNAs are expressed differentially in the human placentas of patients with preeclampsia. Am J Obstet Gynecol 2007;196:261e1–6.
[21] Mouillet JF, Chu T, Hubel CA, Nelson DM, Parks WT, Sadovsky Y. The levels of hypoxia-regulated microRNAs in plasma of pregnant women with fetal growth restriction. Placenta 2010;31:781–4.

Placenta 35 (2014) 787–789

Contents lists available at ScienceDirect

Placenta

journal homepage: www.elsevier.com/locate/placenta

Short communication

Clinical applications of analysis of plasma circulating complete hydatidiform mole pregnancy-associated miRNAs in gestational trophoblastic neoplasia: A preliminary investigation

K. Miura [a, *], Y. Hasegawa [a], S. Abe [a], A. Higashijima [a], S. Miura [a], H. Mishima [b], A. Kinoshita [b], M. Kaneuchi [a], K. Yoshiura [b], H. Masuzaki [a]

[a] Department of Obstetrics and Gynecology, Nagasaki University Graduate School of Biomedical Sciences, 1-7-1 Sakamoto, Nagasaki 852-8501, Japan
[b] Department of Human Genetics, Nagasaki University Graduate School of Biomedical Sciences, Nagasaki, Japan

ARTICLE INFO

Article history:
Accepted 6 June 2014

Keywords:
Complete hydatidiform mole
Gestational trophoblastic neoplasia
miRNAs
Plasma
Molecular marker

ABSTRACT

The aim of this study was to investigate the clinical application of plasma complete hydatidiform mole pregnancy-associated microRNAs (CHM-miRNAs: hsa-miR-520b, hsa-miR-520f and hsa-miR-520c-3p). We measured plasma CHM-miRNA concentration by real-time quantitative reverse transcriptase polymerase chain reaction in two cases of CHM resulting in gestational trophoblastic neoplasia later. As progress of treatments in both cases, the plasma concentrations of CHM-miRNAs showed a decreasing tendency similar to the pattern for serum hCG concentration, but exhibited a transient increasing tendency after each course of chemotherapy, suggesting that the plasma CHM-miRNAs could be an additional follow-up marker for malignant changes of CHM.

© 2014 Elsevier Ltd. All rights reserved.

1. Introduction

Complete hydatidiform mole (CHM) pregnancy-associated miRNAs (CHM-miRNAs; hsa-miR-520b, hsa-miR-520f and hsa-miR-520c-3p) were recently identified in the plasma [1]. The measurement of CHM-miRNAs may be used in clinical management of CHM as a follow-up molecular marker, in addition to the current biochemical marker human chorionic gonadotropin (hCG), which has α- and β-subunits. Malignant change, termed gestational trophoblastic neoplasia (GTN), arises after 15% of cases of CHM pregnancy [2]. Onset of malignant change is signified by a plateaued or rising hCG concentration. However, because GTN generates many other subtypes of hCG, hCG immunoassays fail to or variably detect all hCG variants (e.g. regular hCG, hyperglycosylated hCG and the free beta-subunit of hyperglycosylated hCG, etc.) [3], and therefore are prone to false-negative results [4,5]. Additionally, hCG assays are susceptible to false-positive results, e.g. phantom hCG that is a physiological entity, analytical problem caused by crossreacting heterophilic antibodies [4–6]. Therefore, a new generation of assays for GTN is urgently needed.

In this study, we measured plasma CHM-miRNAs (hsa-miR-520b, hsa-miR-520f and hsa-miR-520c-3p) concentration by real-time quantitative reverse transcriptase polymerase chain reaction (qRT-PCR) in two cases of CHM resulting in GTN later.

2. Materials and methods

2.1. Sample collection

Two cases of CHM resulting in GTN later were analyzed in this study. CHM was diagnosed by pathological, chromosomal and DNA genotyping tests. Serial blood sampling was performed at times, before and after suction evacuation or chemotherapy. Preparation and extraction of total RNA containing small RNA molecules were performed as described previously [7,8].

2.2. Real-time quantitative reverse-transcription polymerase chain reaction (qRT-PCR) analysis

All specific primers and TaqMan probes (hsa-miR-520b, hsa-miR-520f and hsa-miR-520c-3p) were purchased from TaqMan MicroRNA Assays (Applied Biosystems, Warrington, UK). With hCG immunoassay, absolute qRT-PCR analysis was performed to measure the plasma concentrations of CHM-miRNAs as described previously [7,8]. For each miRNA assay, we prepared a calibration curve by 10-fold serial dilution of single-stranded cDNA oligonucleotides corresponding to each miRNA sequence from 1.0×10^2 to 1.0×10^8 copies/mL. Each sample and each calibration dilution was analyzed in triplicate. Each assay could detect down to 10 RNA copies/mL. Every batch of amplifications included three water blanks as negative controls for each of the reverse-transcription and PCR steps. All data were collected and

Abbreviations: CHM, Complete hydatidiform mole; GTN, Gestational trophoblastic neoplasia; qRT-PCR, Quantitative reverse transcriptase polymerase chain reaction; hCG, Human chorionic gonadotropin; MTX, Methotrexate.

* Corresponding author. Tel.: +81 95 819 7363; fax: +81 95 819 7365.
E-mail address: kiyonori@nagasaki-u.ac.jp (K. Miura).

http://dx.doi.org/10.1016/j.placenta.2014.06.004
0143-4004/© 2014 Elsevier Ltd. All rights reserved.

analyzed using the LightCycler® 480 Real-Time PCR System (Roche, Mannheim, Germany).

3. Results and discussion

The first case was a 32-year-old woman with Stage I GTN, which was diagnosed by the International Federation of Gynecology and Obstetrics (FIGO) 2000 staging. In this case, initial chest X-ray indicated no pulmonary lesions, and the first and second evacuations were performed on Days 0 and 7, respectively (Fig. 1A). Serum hCG levels (300, 300 mIU/mL on Day 0) fell to 279 mIU/mL up to Day 38 (Fig. 1A). However, re-elevation of the hCG levels was detected from Day 50 (1004 mIU/mL) to Day 76 (2213 mIU/mL). The visible lesion was confined to the uterus, therefore, a third evacuation was performed on Day 76. After the level of serum hCG had decreased, it rose again from Day 98 (918 mIU/mL) to Day 104 (2720 mIU/mL). Therefore, methotrexate (MTX) therapy was performed on Days 119–123, 142–146, 160–164, and 176–180. Serum hCG concentration on Day 104 (2720 mIU/mL) fell below the detection level (<0.5 mIU/mL) until Day 156 (Fig. 1A). Meanwhile, elevation of three plasma CHM-miRNAs was detected from Day 50 (hsa-miR-520b, hsa-miR-520f and hsa-miR-520c-3p; 1,227, 928 and 520 copies/mL, respectively) to Day 76 (5,862, 3147 and 2541 copies/mL, respectively) and re-elevation was seen from Day 98 (2,215, 1325 and 988 copies/mL, respectively) to Day 104 (9,254, 5543 and 4835 copies/mL, respectively), indicating that measurement of CHM-miRNAs could detect GTN (Fig. 1A). During Days 120–156, the plasma CHM-miRNA concentration showed a decreasing tendency similar to the pattern for serum hCG concentration, but exhibited a transient increase CHM-miRNA concentration after the first course of chemotherapy and then decreased (Fig. 1A). MTX inhibits DNA synthesis, thus, the changing concentration of plasma miRNAs may reflect MTX-induced apoptotic activity.

The second case was a 42-year-old woman with Stage III GTN. In this case, initial chest X-ray indicated no pulmonary lesions, and the first and second evacuations were performed on Days 0 and 7, respectively (Fig. 1B). Serum hCG levels (409,198 mIU/mL at Day 0) fell to 4470 mIU/mL up to Day 22 (Fig. 1B). However, re-elevation of serum hCG concentration were detected on Day 36 (5714 mIU/mL) and Day 41 (6884 mIU/mL). More than 21 lung metastatic lesions <3 cm were identified. MTX, etoposide and actinomycin D therapy was given on Days 43–47, Etoposide and actinomycin D therapy was given on Days 70–73, and then MTX therapy was on Days 83–87, 104–108, 118–122, 127–131, 158–162, and 186–190. Serum hCG levels fell below the detection level of hCG concentration (<0.5 mIU/mL) up to Day 158 (Fig. 1B). Meanwhile, as in the first case, the plasma CHM-miRNA concentrations showed a decreasing tendency, but exhibited a transient tendency after most courses of chemotherapy (Fig. 1B). Two CHM-miRNAs (miR-520b and miR-520f) are at extremely low levels on Day 22 in the second case, while the hCG level indicates that disease is still present. The CHM-miRNAs were cleared rapidly and provided information that is different from that obtained with hCG immunoassay (Fig. 1B). Although CHM-miRNAs seem to be a marker for CHM, of the different markers, miR-520c-3p in particular seems to show a

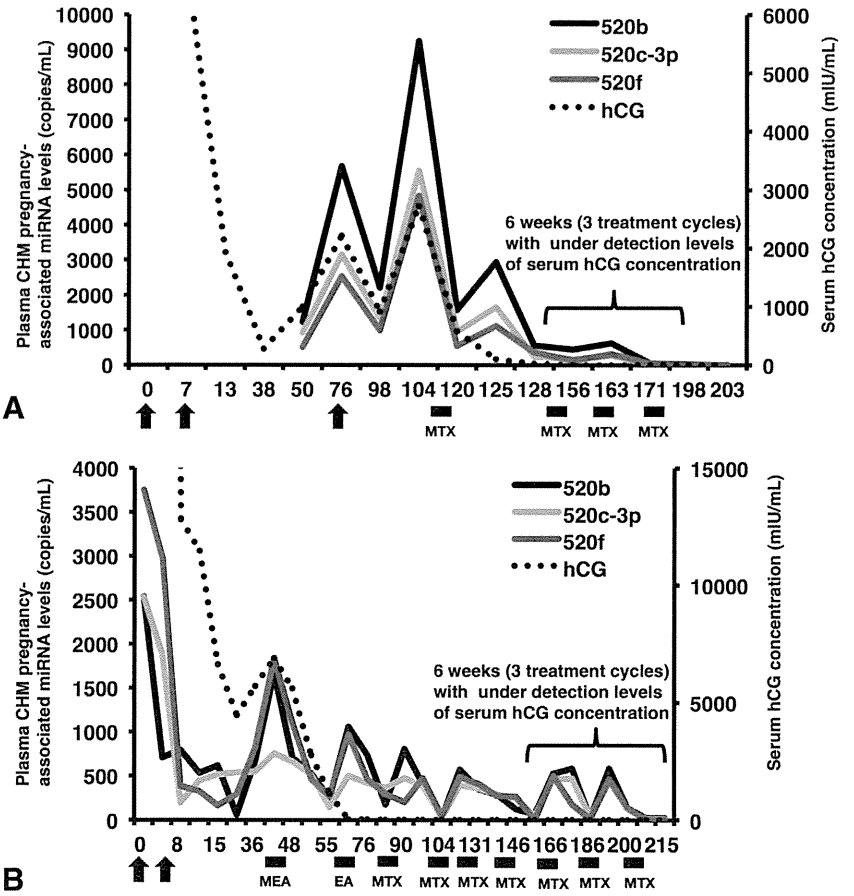

Fig. 1. Changing plasma concentrations of CHM-miRNA in two cases of persistent gestational trophoblastic neoplasia. Black or gray lines indicate the plasma levels of CHM-miRNAs, whereas a broken line indicates serum hCG level. Arrows indicate Days 0 and 7, the days on which evacuations were performed. Black squares indicate the days on which chemotherapy was performed. MEA, combination chemotherapy of MTX, etoposide and actinomycin D; EA, combination chemotherapy of etoposide and actinomycin D.

different pattern of behavior in the two cases. This difference may be attributable to miR-520c-3p in the placental cells, because we have previously reported that MTX therapy shows different circulating levels of β-subunit of hCG (hCGβ) and hPL mRNAs, which are placental mRNAs but expressed from different cells in the placenta [9]. The CHM-miRNAs quantification reflects the molecules from GTN directly, while hCG immunoassay detects the hCG molecule using antibodies. Rapid clearance of plasma CHM-miRNAs may reflect complete elimination of CHM, and the transiently increased concentration of plasma CHM-miRNAs may reflect apoptotic activity induced by therapy. Furthermore, as the merit of different markers, the combination of hCG immunoassay and plural CHM-miRNAs quantification may reduce the risk of false-positive/negative results of hCG immunoassays.

For clinical use of the CHM-miRNAs test, some immediate concerns are to be resolved in further studies. The first concern is that only two cases were analyzed in this study, which is not enough to obtain the definition of markers for GTN, with GTN being such a rare case. Therefore, in future, further cases should be analyzed to evaluate our results. It is also necessary to confirm whether the method is sensitive enough to monitor changes in CHM-miRNA concentration in women with GTN. The second concern is that the conditions and treatments are not the same in these two cases. We chose a different time point for the CHM-miRNA test, which may have affected the results. The transient rise in CHM-miRNA levels does not always appear to reflect the administration of chemotherapy in case 2. Close to the end of MTX therapy, trophoblastic activity in GTN may fall below the detection level of real-time qRT-PCR. However, to explain the transient difference after each course of chemotherapy, it is necessary to measure the plasma concentrations of miRNAs at time points before, after and during chemotherapy. The third concern is that CHM-miRNAs tests were performed only in MTX, EA and MEA therapies for GTN. Therefore, CHM-miRNAs tests should be also evaluated in other chemotherapeutic treatments for GTN. The fourth concern is the cost of combination tests. The cost of CHM-miRNA quantification is about 1000 Japanese yen (JPN), while that of the hCG immunoassay is about 1500 JPN. Therefore, it may be also necessary to reduce the running costs of real-time qRT-PCR.

In conclusion, our results suggest that the measurement of plasma CHM-miRNA concentration by real-time qRT-PCR could be used as an additional follow-up test for GTN, and particularly useful in patients with false-positive/negative results of hCG immunoassay [4–6]. Regarding the evaluation of GTN, CHM-miRNA analysis seems to provide different information in addition to that obtained with hCG immunoassay.

Authors' contribution

All authors confirm that they have contributed to the intellectual content of this paper and have met the following requirements: (1): significant contributions to the conception and design, acquisition of data, or analysis and interpretation of data; (2) drafting or revising the article for intellectual content; and (3) final approval of the published article.

Funding

This work was supported by the Japan Society for the Promotion of Science KAKENHI grant numbers nos. 26462495, 24791712 and 25462563.

Acknowledgments

We would like to thank Dr. Atsushi Yoshida for their technical assistance.

References

[1] Hasegawa Y, Miura K, Furuya K, Yoshiura KI, Masuzaki H. Identification of complete hydatidiform mole pregnancy-associated MicroRNAs in plasma. Clin Chem 2013;59:1410–2.
[2] Seckl MJ, Sebire NJ, Berkowitz RS. Gestational trophoblastic disease. Lancet 2010;376:717–29.
[3] Stenman UH, Alfthan H. Determination of human chorionic gonadotropin. Best Pract Res Clin Endocrinol Metab 2013;27:783–93.
[4] Berkowitz RS, Goldstein DP. Current management of gestational trophoblastic diseases. Gynecol Oncol 2009;112:654–62.
[5] Cole LA. Human chorionic gonadotropin tests. Expert Rev Mol Diagn 2009;9:721–47.
[6] Sturgeon CM, Berger P, Bidart JM, Birken S, Burns C, Norman RJ, et al., IFCC Working Group on hCG. Differences in recognition of the 1st WHO international reference reagents for hCG-related isoforms by diagnostic immunoassays for human chorionic gonadotropin. Clin Chem 2009;55:1484–91.
[7] Miura K, Miura S, Yamasaki K, Higashijima A, Kinoshita A, Yoshiura K, et al. Identification of pregnancy-associated microRNAs in maternal plasma. Clin Chem 2010;56:1767–71.
[8] Higashijima A, Miura K, Mishima H, Kinoshita A, Jo O, Abe S, et al. Characterization of placenta-specific microRNAs in fetal growth restriction pregnancy. Prenat Diagn 2013;33:214–22.
[9] Masuzaki H, Miura K, Yoshiura K, Yamasaki K, Miura S, Yoshimura S, et al. Placental mRNA in maternal plasma and its clinical application to the evaluation of placental status in a pregnant woman with placenta previa-percreta. Clin Chem 2005;51:923–5.

Journal of Medical Virology 86:1153–1158 (2014)

Genome-Wide Association Study of HPV-Associated Cervical Cancer in Japanese Women

Kiyonori Miura,[1] Hiroyuki Mishima,[2] Akira Kinoshita,[2] Chisa Hayashida,[2] Shuhei Abe,[1] Katsushi Tokunaga,[3] Hideaki Masuzaki,[1] and Koh-ichiro Yoshiura[2]*

[1]*Department of Obstetrics and Gynecology, Graduate School of Biomedical Sciences, Nagasaki University, Nagasaki, Japan*
[2]*Department of Human Genetics, Graduate School of Biomedical Sciences, Nagasaki University, Nagasaki, Japan*
[3]*Department of Human Genetics, Graduate School of Medicine, The University of Tokyo, Tokyo, Japan*

One of the important factors influencing the development of uterine cervical cancer is human papillomavirus infection in women. Usually, the infecting papillomavirus is eliminated from individuals; however, some retain the virus and this is believed to lead to the development of uterine cervical cancer. It is possible that virus elimination or persistent infection depends on an individual's genetic background. To identify single nucleotide polymorphisms associated with susceptibility to persistent infection or cervical cancer, a genome-wide association study was performed on 226 cases and 186 controls. Some of the single nucleotide polymorphisms showed a *P*-value $< 10^{-5}$; however, no polymorphisms that were significantly associated with susceptibility to cervical cancer were identified. ***J. Med. Virol. 86:1153–1158, 2014.***

© 2014 Wiley Periodicals, Inc.

KEY WORDS: uterine cervical cancer; susceptibility; GWAS; human papilloma virus

INTRODUCTION

Uterine cervical cancer is a worldwide problem, especially in developing countries, where it is the first or second most common cancer in women [Arbyn et al., 2011]. Persistent infections with oncogenic human papillomavirus (HPV) are recognized as a major cause of uterine cervical cancer. Individuals with oncogenic HPV infection have a risk of cervical cancer with an odds ratio over 100 [Muñoz et al., 2003]. Although, genital infections with HPV are very common, HPV disappears naturally in most cases within a relatively short period and carries little risk of developing the disease [Moscicki et al., 1993; Ho et al., 1998; Woodman et al., 2001]. Within populations, it is thought that some individuals have persistent infections and a high risk for cervical cancer. The pathological process that results in oncogenic HPV persistent infection developing into invasive cervical cancer is not fully understood; however, epidemiological evidence indicates clearly that different viral characteristics and oncogenic HPV genotypes are associated with variable risk of cervical cancer [Muñoz et al., 2003]. HPV types 16 and 18, 31, 33, 35, 39, 45, 51, 52, 56, 58, 59, 68, 73, and 82 are classified as oncogenic high-risk viral types for cervical cancer [Muñoz et al., 2003]. Additional cofactors for cervical cancer, for example, environmental factors (including oral contraceptive use and smoking), have been identified as risk factors [Castellsague and Munoz, 2003]. In addition to the viral genotype and environmental factors, the genotype of an individual could be a risk factor for cervical cancer [Habbous et al., 2012; Matsumoto et al., 2012; Safaeian et al., 2012; Wang et al., 2013; Zhao et al., 2013], because a persistent infection could be defined by the interaction between the pathogen (HPV) and the host (individual). Thus, it is hypothesized that host genetic factors are involved in uterine cervical carcinogenesis. To evaluate the possible effect of an individual genotype on cervical cancer development, a genome-wide association study in Japanese women was performed.

Grant sponsor: Ministry of Health, Labour, and Welfare, Japan (to K.Y. and H.M.)

*Correspondence to: Koh-ichiro Yoshiura, Department of Human Genetics, Graduate School of Biomedical Sciences, Nagasaki University, 1-12-4 Sakamoto, Nagasaki 852-8523, Japan. E-mail: kyoshi@nagasaki-u.ac.jp

Accepted 11 March 2014

DOI 10.1002/jmv.23943
Published online 4 April 2014 in Wiley Online Library (wileyonlinelibrary.com).

© 2014 WILEY PERIODICALS, INC.

MATERIALS AND METHODS

Subjects and Samples

The study participants were 226 unrelated Japanese women with cancer of the uterine cervix, or carcinoma in situ, from the Nagasaki prefecture. Experienced pathologists from the Division of Pathology at Nagasaki University Hospital confirmed the diagnoses, before or after surgery. One hundred eighty-six Japanese general individuals (125 males and 61 females) were examined as the control group. In addition, SNP data from 234 Japanese individuals from the Human Genome Variation Database <https://gwas.biosciencedbc.jp/index.html> were analyzed as the general population. All samples were obtained after receiving written informed consent, and the Institutional Review Board for Ethical, Legal, and Social Issues of Nagasaki University approved the study protocol.

Genotyping

Allele calling from the Affymetrix Genome-Wide Human SNP Array 6.0 (Affy6.0; Affymetrix, Santa Clara, CA) was performed using Affymetrix Power Tools version 1.15.0 (http://www.affymetrix.com/partners_programs/programs/developer/tools/powertools.affx). To ensure precise allele calling, 1,679 Affy6.0 raw signal data (CEL files) derived from samples in this study and HapMap3 diverse populations (available at: ftp://ftp.ncbi.nlm.nih.gov/hapmap/raw_data/hapmap3_affy6.0/) were processed simultaneously (Table I). The IGG3 software [Purcell et al., 2007; Li et al., 2009] was used to merge the allele-called data (CHP files) of the HPV and control population datasets. The genome-wide association calculation was computed using the PLINK software [Li et al., 2007] for 226 cases and 186 (125 males and 61 females) general Japanese controls on autosomal and X chromosomes. The total genotyping rate was 0.984, and 556,045 SNPs that were called in >95% of samples and had minor allele frequencies >5% were used for analysis. A Manhattan plot and a quantile–quantile plot (QQ plot) were generated using R scripts based on the qqman.r script (https://github.com/stephenturner/qqman). The genomic inflation factor (λ) was calculated and used to assess the presence of systematic bias in the observed test statistics [Aulchenko et al., 2007]. SNPs with $P < 10^{-4}$ were annotated using WGAViewer [Ge et al., 2008] with the homo_sapiens_core_46_36h, homo_sapiens_variation_46_36h, and ensembl_ontology_46 databases.

TABLE I. Datasets Used for Allele Calling

Datasets	Population	Number of CEL files
HPV affected + unaffected	Japanese	243
Controls	Japanese	189
HapMap3	ASW	87
HapMap3	CEU	177
HapMap3	CHB	89
HapMap3	CHD	90
HapMap3	GIH	90
HapMap3	JPT	91
HapMap3	LWK	90
HapMap3	MXL	84
HapMap3	MKK	179
HapMap3	TSI	90
HapMap3	YRI	180
Total		1,679

CEL file, raw sequence data file; ASW, African ancestry in Southwest USA; CEU, Utah residents with Northern and Western European ancestry from the CEPH collection; CHB, Han Chinese in Beijing, China; CHD, Chinese in Metropolitan Denver, Colorado; GIH, Gujarati Indians in Houston, Texas; JPT, Japanese in Tokyo, Japan; LWK, Luhya in Webuye, Kenya; MXL, Mexican ancestry in Los Angeles, California; MKK, Maasai in Kinyawa, Kenya; TSI, Toscani in Italia; YRI, Yoruba in Ibadan, Nigeria.

RESULTS

SNPs with a P-value $< 10^{-4}$ showed relatively lower bias for their observed test statistics in the QQ plot (Fig. 1). The genomic inflation factor was 1.148, indicating that the observed test statistics were not particularly inflated by a systematic bias, such as population stratification. The genome-wide association study results were plotted and shown in Figure 2. Eighty-nine SNPs with a P-value $< 10^{-4}$ were annotated (Table II). In the QQ plot and the Manhattan plot, SNPs showing an incoherent signal plot with a P-value $< 10^{-4}$ were removed after visual inspection. SNPs showing a P-value $< 5 \times 10^{-5}$ were genotyped by sequencing in 192 Japanese women without cervical cancer that were different from the general

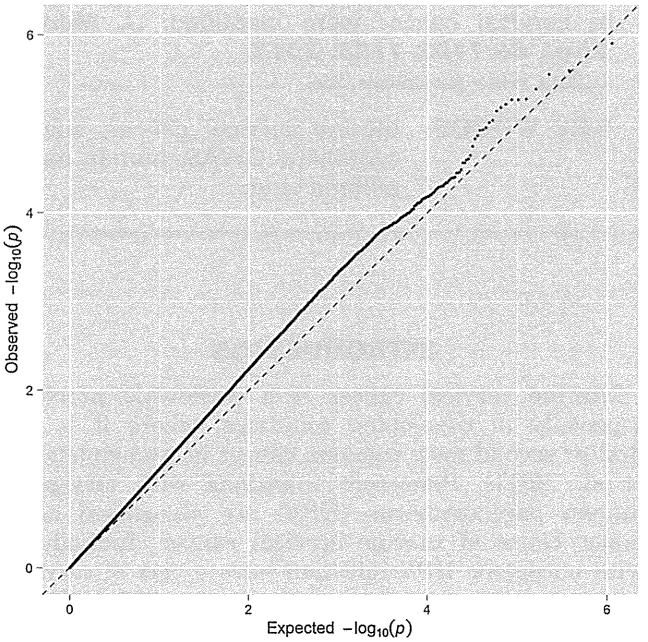

Fig. 1. Quantile–quantile plot (QQ plot) of 556,045 SNPs that were called among >95% samples and that had minor allele frequencies >5%.

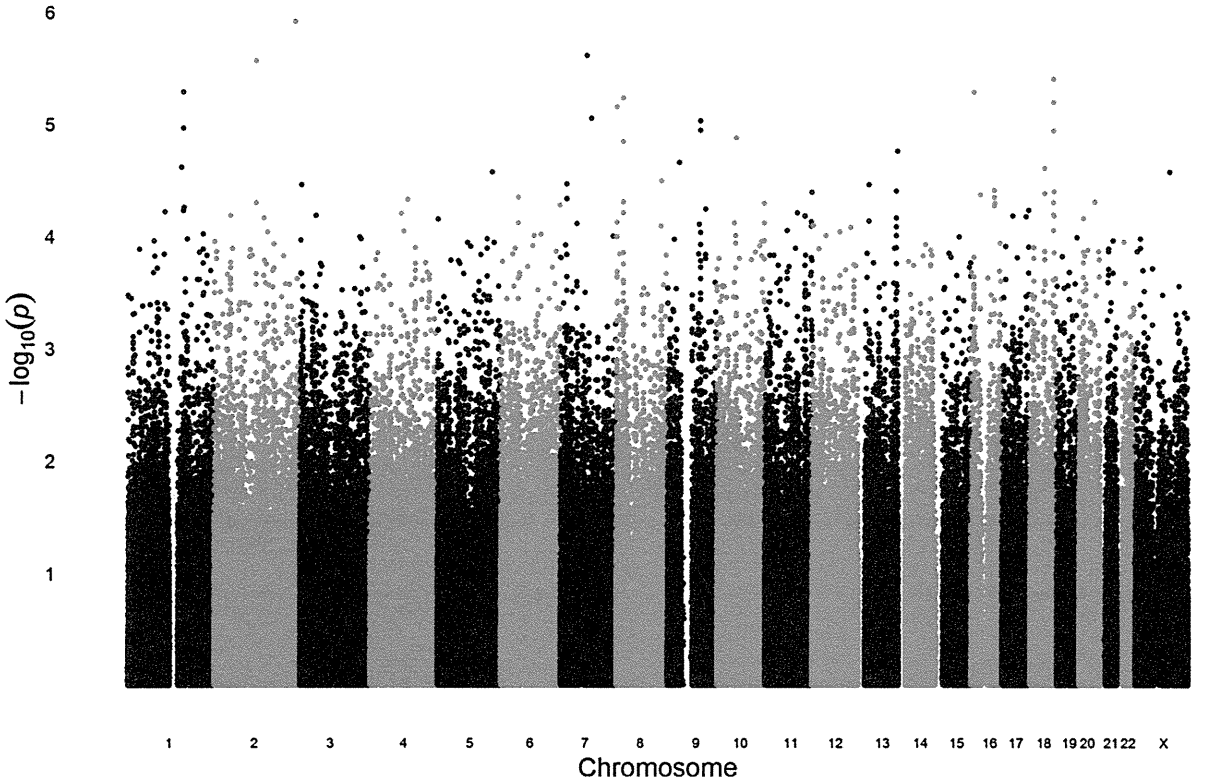

Fig. 2. Manhattan plot of the genome-wide association study. SNPs showing incoherent signal clustering plots in genotyping and with P-values $< 10^{-4}$ were removed from this Manhattan plot by visual inspection. SNPs with lower P-values are listed in Table II.

population group in the initial genome-wide association screening and genotyping of the 226 cervical cancer subjects was repeated for confirmation. Analysis of the sequencing genotype data indicated that none of the SNPs with a P-value $< 5 \times 10^{-5}$ showed a significant association (data not shown).

After the initial genome-wide association screening using SNP6.0 genotyping, a mimic replication genome-wide association study was performed using the Human Genome Variation Database as second Japanese control samples. Among 89 SNPs showing a P-value $< 10^{-4}$ in the initial genome-wide association screening, two SNPs, rs621310 (P-value $= 6.24 \times 10^{-5}$) and rs11653282 (P-value $= 6.69 \times 10^{-5}$), showed a weak association with P-values of 3.90×10^{-4} and 7.57×10^{-5}, respectively, compared with the SNP data set from the Human Genome Variation Database.

DISCUSSION

In this study, SNPs with lower P-values in a genome-wide association study of cervical cancer susceptibility loci were identified and are shown in Table II. Over 500,000 SNPs were genotyped and used for statistical calculation; therefore, a truly associated SNP should have a P-value $< 1.0 \times 10^{-7}$, according to conservative Bonferroni correction. However, no SNPs that were significantly associated with cervical cancer were identified, even when a slight inflation in the QQ plot was allowed. After the initial SNP6.0 screening, none of the SNPs with P-values $< 5 \times 10^{-5}$ showed a significant association when compared with the second control group, although, those SNPs in Table II could have a small effect on the development of cervical cancer or persistent viral infection. Two SNPs, rs621310 and rs11653282 with P-values 6.24×10^{-5} and 6.69×10^{-5} in the first screening set, respectively, showed a slight association compared with second independent control sample groups. Thus, rs621310 and rs11653282 may have some effect on the development of cervical cancer.

Generally, it is thought that HPV disappears naturally in most cases within a relatively short period; however, persistent infection with oncogenic HPV confers a risk of developing cervical cancer [Moscicki et al., 1993; Ho et al., 1998; Woodman et al., 2001]. Different HPV genotypes are associated with different grades of risk for cervical cancer [Stoler et al., 2011; Wright et al., 2011]. Thus, both persistent infection and viral genotype generate a different degree of cervical cancer risk. An individual's predisposition for persistent infection or viral removal could affect cervical cancer development, because the relationship between the viral genotype and an individual's immunological reactions could

TABLE II. Single Nucleotide Polymorphisms (SNPs) With P-Values $< 10^{-4}$

SNP[a]	CHR	Position[b]	Minor allele	Freq. in cases[c]	Freq. in cont[d]	Major allele	CHISQ[e]	P[f]	OR[g]	SE[h]	L95[i]	U95[j]	Gene[k]	Effect[l]
rs997363	2	228,217,702	C	0.57300	0.40320	T	23.53	1.23E−06	1.9860	0.1422	1.5030	2.6240		
rs7780883	7	76,900,648	A	0.15710	0.05376	G	22.17	2.49E−06	3.2800	0.2637	1.9560	5.5000		
rs6726538	2	118,605,699	A	0.55130	0.38710	T	21.98	2.76E−06	1.9460	0.1427	1.4710	2.5730		
rs8088832	18	68,077,737	T	0.33330	0.49190	C	21.26	4.02E−06	0.5164	0.1441	0.3894	0.6849		
rs12068654	1	159,010,373	G	0.03319	0.11480	T	20.76	5.22E−06	0.2648	0.3096	0.1443	0.4858		
rs4782151	16	9,233,486	T	0.37390	0.53230	C	20.72	5.32E−06	0.5248	0.1423	0.3971	0.6936		
rs4782152	16	9,233,512	G	0.37390	0.53230	A	20.72	5.32E−06	0.5248	0.1423	0.3971	0.6936		
rs11985951	8	20,636,789	C	0.04222	0.12900	T	20.5	5.96E−06	0.2976	0.2808	0.1716	0.5160		
rs7238505	18	68,063,042	C	0.33110	0.48640	T	20.33	6.52E−06	0.5227	0.1446	0.3937	0.6939		
rs6558578	8	1,957,133	T	0.12000	0.23920	G	20.15	7.15E−06	0.4336	0.1892	0.2992	0.6283		
rs3899697	7	88,437,721	A	0.42950	0.27870	T	19.71	9.01E−06	1.9490	0.1512	1.4490	2.6210	ZNF804B	Intron
rs16907273	9	93,010,186	T	0.13720	0.25950	C	19.6	9.57E−06	0.4537	0.1810	0.3182	0.6469		
rs11582702	1	158,994,610	T	0.03829	0.12020	C	19.34	1.10E−05	0.2914	0.2950	0.1634	0.5194		
rs16907269	9	93,010,093	C	0.13720	0.25810	T	19.24	1.15E−05	0.4571	0.1809	0.3206	0.6516		
rs8085971	18	68,068,143	A	0.34820	0.50000	T	19.21	1.17E−05	0.5342	0.1437	0.4031	0.7080		
rs10825123	10	55,281,166	G	0.07176	0.17120	T	18.95	1.34E−05	0.3743	0.2322	0.2374	0.5899	PCDH15	Intron
rs1450291	8	20,637,771	G	0.33710	0.48650	A	18.78	1.47E−05	0.5367	0.1443	0.4045	0.7120		
rs9603948	13	112,486,021	A	0.39060	0.24720	C	18.42	1.77E−05	1.9530	0.1570	1.4350	2.6560	ATP11A	Intron
rs1856195	9	33,686,330	A	0.38070	0.52960	G	17.97	2.24E−05	0.5462	0.1432	0.4125	0.7232		
rs4971066	1	153,372,506	T	0.05381	0.13980	G	17.79	2.47E−05	0.3500	0.2577	0.2112	0.5799	EFNA1	Intron
rs17798773	18	43,361,903	A	0.03540	0.11020	G	17.74	2.53E−05	0.2963	0.3037	0.1634	0.5372		
rs768198	23	99,651,741	C	0.30220	0.46150	G	17.6	2.73E−05	0.5053	0.1638	0.3666	0.6966		
rs17054397	5	156,613,454	G	0.03556	0.11020	A	17.59	2.74E−05	0.2976	0.3037	0.1641	0.5397	ITK	UTR
rs2020247	8	129,154,195	G	0.28980	0.16670	C	17.26	3.27E−05	2.0400	0.1735	1.4520	2.8670	PVT1	Intron
rs6461425	7	19,358,611	G	0.22350	0.35410	C	17.13	3.49E−05	0.5250	0.1567	0.3861	0.7138		
rs4769045	13	30,157,630	C	0.02222	0.08602	T	17.1	3.55E−05	0.2415	0.3694	0.1171	0.4981		
rs769626	3	3,793,605	G	0.20350	0.33060	T	17.1	3.56E−05	0.5173	0.1606	0.3776	0.7087		
rs9933029	16	66,860,911	A	0.13390	0.24590	G	16.89	3.96E−05	0.4741	0.1839	0.3306	0.6799	SLC7A6	Intron
rs4238266	13	108,779,132	T	0.16370	0.28230	A	16.86	4.02E−05	0.4978	0.1715	0.3557	0.6968		
rs9948124	18	69,710,118	G	0.20890	0.33600	A	16.84	4.06E−05	0.5218	0.1597	0.3815	0.7135		
rs11600687	11	134,126,220	A	0.25000	0.38320	G	16.82	4.11E−05	0.5366	0.1526	0.3979	0.7238		
rs17736813	18	43,361,984	C	0.03540	0.10750	G	16.76	4.24E−05	0.3046	0.3046	0.1676	0.5534		
rs11648276	16	26,983,256	T	0.56550	0.41940	C	16.71	4.36E−05	1.8020	0.1446	1.3570	2.3930		
rs7761173	6	50,191,241	C	0.49560	0.35410	T	16.61	4.60E−05	1.7920	0.1438	1.3520	2.3760		
rs9935025	16	66,864,948	T	0.13720	0.24860	C	16.61	4.60E−05	0.4804	0.1821	0.3362	0.6864	SLC7A6	Intron
rs11768982	7	19,319,632	G	0.43530	0.57800	A	16.55	4.73E−05	0.5628	0.1418	0.4263	0.7431		
rs2301718	4	106,229,212	G	0.30750	0.18380	A	16.53	4.78E−05	1.9720	0.1685	1.4170	2.7440		
rs4239650	20	45,761,292	C	0.26380	0.39780	T	16.44	5.03E−05	0.5422	0.1518	0.4027	0.7301	SULF2	Intron
rs2597419	8	20,639,046	T	0.29420	0.43010	C	16.44	5.03E−05	0.5524	0.1470	0.4141	0.7369		
rs7232482	18	68,058,704	G	0.38790	0.52970	T	16.42	5.06E−05	0.5626	0.1425	0.4255	0.7438		
rs17047801	2	118,603,973	T	0.40930	0.27420	C	16.41	5.11E−05	1.8340	0.1505	1.3660	2.4640		
rs8049057	16	67,768,162	T	0.09735	0.02703	G	16.39	5.15E−05	3.8820	0.3577	1.9260	7.8270		
rs4131689	10	133,594,318	A	0.43050	0.57260	C	16.38	5.18E−05	0.5643	0.1419	0.4273	0.7452		
rs17787659	6	169,191,138	T	0.17190	0.29030	C	16.32	5.35E−05	0.5073	0.1695	0.3639	0.7073		
rs4783552	16	66,867,813	T	0.13720	0.24730	C	16.29	5.43E−05	0.4838	0.1820	0.3387	0.6913	SLC7A6	Intron
rs10917638	1	161,147,761	C	0.11500	0.03693	T	16.25	5.56E−05	3.3900	0.3188	1.8150	6.3320		
rs16912217	9	108,916,731	T	0.05357	0.13440	C	16.18	5.77E−05	0.3645	0.2591	0.2194	0.6057		
rs17313034	1	158,980,472	C	0.03319	0.10220	T	16.13	5.93E−05	0.3017	0.3135	0.1632	0.5577	SLAMF7	Intron
rs7220348	17	76,500,453	A	0.41330	0.55410	C	16.12	5.95E−05	0.5671	0.1418	0.4295	0.7487	RPTOR	Intron
rs10785799	1	106,993,008	G	0.42220	0.56450	A	16.07	6.11E−05	0.5636	0.1435	0.4254	0.7467		
rs621310	11	92,422,987	G	0.32080	0.45700	A	16.03	6.24E−05	0.5612	0.1449	0.4225	0.7455		
rs17493092	8	20,577,223	A	0.02691	0.09218	C	16.01	6.29E−05	0.2723	0.3450	0.1385	0.5354		
rs7691791	4	88,505,433	T	0.36640	0.23460	C	16	6.32E−05	1.8860	0.1596	1.3790	2.5790	HSD17B11	Intron
rs11876001	18	68,091,531	T	0.39560	0.53490	C	15.94	6.55E−05	0.5689	0.1418	0.4309	0.7511		
rs7624805	3	46,438,428	G	0.38460	0.25270	A	15.93	6.56E−05	1.8480	0.1548	1.3650	2.5030		
rs6742593	2	46,744,042	C	0.08444	0.17740	T	15.93	6.58E−05	0.4276	0.2172	0.2794	0.6545		
rs9957017	18	69,711,096	C	0.21210	0.33600	T	15.91	6.64E−05	0.5318	0.1594	0.3891	0.7268		
rs1980306	11	114,171,705	A	0.11500	0.21770	T	15.9	6.68E−05	0.4670	0.1937	0.3195	0.6827		
rs11653282	17	31,260,859	T	0.45630	0.31720	C	15.9	6.69E−05	1.8070	0.1490	1.3490	2.4190		
rs1872080	17	69,022,931	G	0.48890	0.35050	A	15.88	6.75E−05	1.7730	0.1442	1.3360	2.3510	SDK2	Intron
rs4134382	13	108,755,291	T	0.35620	0.49460	C	15.83	6.92E−05	0.5652	0.1439	0.4263	0.7494		
rs592398	13	108,677,223	G	0.20800	0.33060	A	15.83	6.93E−05	0.5315	0.1599	0.3885	0.7272		
rs10196730	2	139,631,288	C	0.10840	0.03495	A	15.83	6.94E−05	3.3580	0.3203	1.7920	6.2910		
rs6134537	20	12,326,641	G	0.18580	0.08871	C	15.8	7.03E−05	2.3450	0.2188	1.5270	3.6010		
rs4866625	5	2,224,041	G	0.29050	0.42500	C	15.78	7.10E−05	0.5541	0.1493	0.4135	0.7424		
rs10507390	13	30,157,072	A	0.02434	0.08602	G	15.7	7.43E−05	0.2650	0.3569	0.1317	0.5334		
rs2279694	11	133,025,417	T	0.19470	0.31450	C	15.68	7.51E−05	0.5269	0.1630	0.3828	0.7253		

TABLE II. (*Continued*)

SNP[a]	CHR	Position[b]	Minor allele	Freq. in cases[c]	Freq. in cont[d]	Major allele	CHISQ[e]	P[f]	OR[g]	SE[h]	L95[i]	U95[j]	Gene[k]	Effect[l]
rs11136457	8	1,985,400	A	0.19250	0.31180	G	15.66	7.60E−05	0.5260	0.1636	0.3817	0.7249	MYOM2	Intron
rs2814191	10	133,921,838	G	0.47290	0.33600	A	15.63	7.70E−05	1.7720	0.1453	1.3330	2.3570	STK32C	Intron
rs11101565	10	49,796,881	C	0.45800	0.32260	T	15.63	7.72E−05	1.7740	0.1457	1.3340	2.3600	WDFY4	Intron
rs2671702	10	49,805,164	G	0.45800	0.32260	A	15.63	7.72E−05	1.7740	0.1457	1.3340	2.3600	WDFY4	Intron
rs41402445	6	50,194,198	G	0.52270	0.38380	A	15.62	7.73E−05	1.7590	0.1433	1.3280	2.3290		
rs2686838	7	47,973,174	T	0.41200	0.55280	C	15.59	7.85E−05	0.5670	0.1442	0.4274	0.7521	HUS1	Intron
rs10868580	9	89,230,294	C	0.12830	0.04839	G	15.57	7.94E−05	2.8950	0.2796	1.6740	5.0080		
rs16930370	12	3,257,958	C	0.17790	0.08333	T	15.53	8.12E−05	2.3810	0.2249	1.5320	3.7000	TSPAN9	CDS
rs4422742	8	127,362,178	C	0.26730	0.39780	T	15.5	8.23E−05	0.5521	0.1516	0.4102	0.7431		
rs12290536	11	132,965,083	A	0.03319	0.10050	G	15.5	8.27E−05	0.3071	0.3146	0.1657	0.5689		
rs9521234	13	108,675,959	T	0.21330	0.33610	C	15.48	8.32E−05	0.5358	0.1596	0.3918	0.7326		
rs11614063	12	111,510,044	A	0.05333	0.13170	G	15.46	8.41E−05	0.3714	0.2598	0.2232	0.6180		
rs1195958	11	64,693,386	C	0.42270	0.28960	T	15.32	9.06E−05	1.7960	0.1503	1.3380	2.4120		
rs8097717	18	68,064,038	A	0.39560	0.53260	G	15.32	9.06E−05	0.5743	0.1422	0.4346	0.7588		
rs3775018	4	96,062,889	T	0.07045	0.15680	C	15.31	9.14E−05	0.4077	0.2348	0.2573	0.6460	BMPR1B	Intron
rs12819209	12	79,894,979	T	0.06667	0.15050	C	15.29	9.21E−05	0.4031	0.2382	0.2527	0.6429		
rs289932	2	151,714,271	C	0.41670	0.55430	T	15.28	9.25E−05	0.5742	0.1424	0.4344	0.7590		
rs12238387	9	93,074,389	G	0.14930	0.25960	A	15.25	9.42E−05	0.5007	0.1790	0.3526	0.7111	AUH	Intron
rs1025652	1	215,148,762	T	0.34960	0.48390	A	15.22	9.59E−05	0.5732	0.1432	0.4330	0.7589	ESRRG	Intron
rs4348786	1	215,148,906	C	0.34960	0.48390	T	15.22	9.59E−05	0.5732	0.1432	0.4330	0.7589	ESRRG	Intron
rs7758085	6	114,700,253	A	0.34030	0.47570	T	15.19	9.72E−05	0.5685	0.1454	0.4275	0.7560		
rs1194713	10	53,867,696	G	0.28760	0.17200	A	15.14	9.98E−05	1.9430	0.1722	1.3860	2.7230		

[a]The dbSNP rs number.
[b]The NCBI Build 36-genome assembly.
[c]Minor allele frequencies in controls.
[d]Minor allele frequencies in cases.
[e]Chi-square value.
[f]P-value calculated by chi square statistics.
[g]Odds ratio.
[h]Standard error.
[i]Upper 95% confidence interval.
[j]Lower 95% confidence interval.
[k]RefSeq genes encompassing the SNP locus.
[l]RefSeq gene annotation.

affect virus removal. In this study, a genome-wide association study in a Japanese population could not identify susceptibility loci for cervical cancer. However, two other genome-wide association studies in other populations did identify cervical cancer susceptibility loci. One genome-wide association study in the Han Chinese population identified strong associations between cervical cancer and three loci: 4q12 (rs13117307), 17q12 (rs8067378), and 6p21.32 (rs4282438 and rs9272143) [Shi et al., 2013]. The other genome-wide association study (in a Swedish population) found three cervical cancer susceptibility loci at 6p21.32 (rs2516448, rs9272143, and rs3117027) [Chen et al., 2013]. The DPB1–DPB2 locus was included in these two genome-wide association studies; therefore, this locus might be a susceptibility determinant for HPV viral infection followed by cervical cancer development. SNPs rs13117307, rs8067378, and rs4282438 are not included in Affy6.0, and rs9272143 was excluded during the calculation process. Analysis of the SNP data on the 100 kb region that include those SNPs in this study showed that none of them showed a P-value < 0.001. The minor allele frequencies for rs4282439 were 0.35 and 0.41 for the case and control data, respectively, in the Han Chinese study [Shi et al., 2013], and this would correspond to a P-value of about 2.5×10^{-4} in the present study. The relatively small sample numbers (226 cases and 186 controls) in the present study may explain the higher P-value compared with the previous study. It may be difficult to detect SNPs with small effects on cervical cancer development or persistent viral infection. The purpose of this study was to identify SNPs that are associated significantly with cervical cancer development, with the ultimate aim of identifying predictive markers. However, no SNPs that were associated significantly were identified, even in the DPB1–DPB2 locus.

Genetic polymorphisms in several genes have been reported as cervical cancer susceptibility loci by candidate gene association study [Habbous et al., 2012; Matsumoto et al., 2012; Safaeian et al., 2012; Wang et al., 2013; Zhao et al., 2013]. For example, in a previous study of Japanese women, an association between the copy number of the defensin beta 4 gene and cervical cancer was reported, but its effect on predisposition to cervical cancer was small [Abe et al., 2013]. However, none of the candidate-associated genes were included in the genome-wide association study; therefore, further replicative studies should be performed. If the persistent infection is defined by the interaction between viral and individual genotypes, SNPs predisposing to cervical cancer might be found using denser or lower-frequency SNP

genotyping, and using more cases and controls. Therefore, samples of cervical cancer are being collected continuously for subsequent genotyping to identify SNPs that predispose women to cervical cancer.

ACKNOWLEDGMENTS

The authors would like to thank the affected individuals and the families for contributing samples for this study. Also, the authors would like to thank Shoko Miura and Ai Higashijima for their assistance in this study.

REFERENCES

Abe S, Miura K, Kinoshita A, Mishima H, Miura S, Yamasaki K, Hassegawa Y, Higashijima A, Jo O, Yoshida A, Yoshiura K, Masuzaki H. 2013. Copy number variation of the antimicrobial-gene, defensin beta 4, is associated with susceptibility to cervical cancer. J Hum Genet 58:250–253.

Arbyn M, Castellsagué X, de Sanjosé S, Bruni L, Saraiya M, Bray F, Ferlay J. 2011. Worldwide burden of cervical cancer in 2008. Ann Oncol 22:2675–2686.

Aulchenko YS, Ripke S, Isaacs A, van Duijn CM. 2007. GenABEL: An R library for genome-wide association analysis. Bioinformatics 23:1294–1296.

Castellsague X, Munoz N. 2003. Cofactors in human papillomavirus carcinogenesis-role of parity, oral contraceptives, and tobacco smoking. J Natl Cancer Inst Monogr 31:20–28.

Chen D, Juko-Pecirep I, Hammer J, Ivansson E, Enroth S, Gustavsson I, Feuk L, Magnusson PK, McKay JD, Wilander E, Gyllensten U. 2013. Genome-wide association study of susceptibility loci for cervical cancer. J Natl Cancer Inst 105:624–633.

Ge D, Zhang K, Need AC, Martin O, Fellay J, Urban TJ, Telenti A, Goldstein DB. 2008. WGAViewer: Software for genomic annotation of whole genome association studies. Genome Res 18:640–643.

Habbous S, Pang V, Eng L, Xu W, Kurtz G, Liu FF, Mackay H, Amir E, Liu G. 2012. p53 Arg72Pro polymorphism, HPV status and initiation, progression, and development of cervical cancer: A systematic review and meta-analysis. Clin Cancer Res 18: 6407–6415.

Ho GY, Bierman R, Beardsley L, Chang CJ, Burk RD. 1998. Natural history of cervicovaginal papillomavirus infection in young women. N Engl J Med 338:423–428.

Li M-X, Jiang L, Ho S-L, Song Y-Q, Sham P-C. 2007. IGG: A tool to integrate GeneChips for genetic studies. Bioinformatics 23: 3105–3107.

Li M-X, Jiang L, Kao PY-P, Sham P-C, Song Y-Q. 2009. IG G3: A tool to rapidly integrate large genotype datasets for whole-genome imputation and individual-level meta-analysis. Bioinformatics 25:1449–1450.

Matsumoto K, Maeda H, Oki A, Takatsuka N, Yasugi T, Furuta R, Hirata R, Mitsuhashi A, Fujii T, Hirai Y, Iwasaka T, Yaegashi N, Watanabe Y, Nagai Y, Kitagawa T, Yoshikawa H, for Japan HPV and Cervical Cancer (JHACC) Study Group. 2012. HLA class II DRB1*1302 allele protects against progression to cervical intraepithelial neoplasia grade 3: A multicenter prospective cohort study. Int J Gynecol Cancer 22:471–478.

Moscicki AB, Palefsky J, Smith G, Siboshski S, Schoolnik G. 1993. Variability of human papillomavirus DNA testing in a longitudinal cohort of young women. Obstet Gynecol 82:578–585.

Muñoz N, Bosch FX, de Sanjosé S, Herrero R, Castellsagué X, Shah KV, Snijders PJF, Meijer CJLM. 2003. Epidemiologic classification of human papillomavirus types associated with cervical cancer. N Engl J Med 348:518–527.

Purcell S, Neale B, Todd-Brown K, Thomas L, Ferreira MA, Bender D, Maller J, Sklar P, de Bakker PI, Daly MJ, Sham PC. 2007. PLINK: A tool set for whole-genome association and population-based linkage analyses. Am J Hum Genet 81:559–575.

Safaeian M, Hildesheim A, Gonzalez P, Yu K, Porras C, Li Q, Rodriguez AC, Sherman ME, Schiffman M, Wacholder S, Burk R, Herrero R, Burdette L, Chanock SJ, Wang SS. 2012. Single nucleotide polymorphisms in the PRDX3 and RPS19 and risk of HPV persistence and cervical precancer/cancer. PLoS ONE 7: e33619.

Shi Y, Li L, Hu Z, Li S, Wang S, Liu J, Wu C, He L, Zhou J, Li Z, Hu T, Chen Y, Jia Y, Wang S, Wu L, Cheng X, Yang Z, Yang R, Li X, Huang K, Zhang Q, Zhou H, Tang F, Chen Z, Shen J, Jiang J, Ding H, Xing H, Zhang S, Qu P, Song X, Lin Z, Deng D, Xi L, Lv W, Han X, Tao G, Yan L, Han Z, Li Z, Miao X, Pan S, Shen Y, Wang H, Liu D, Gong E, Li Z, Zhou L, Luan X, Wang C, Song Q, Wu S, Xu H, Shen J, Qiang F, Ma G, Liu L, Chen X, Liu J, Wu J, Shen Y, Wen Y, Chu M, Yu J, Hu X, Fan Y, He H, Jiang Y, Lei Z, Liu C, Chen J, Zhang Y, Yi C, Chen S, Li W, Wang D, Wang Z, Di W, Shen K, Lin D, Shen H, Feng Y, Xie X, Ma D. 2013. A genome-wide association study identifies two new cervical cancer susceptibility loci at 4q12 and 17q12. Nat Genet 45:918–922.

Stoler MH, Wright TC Jr, Sharma A, Apple R, Gutekunst K, Wright TL. 2011. ATHENA (Addressing THE Need for Advanced HPV Diagnostics) HPV Study Group. High-risk human papillomavirus testing in women with ASC-US cytology: Results from the ATHENA HPV study. Am J Clin Pathol 135:468–475.

Wang M, Chu H, Wang S, Wang M, Wang W, Han S, Zhang Z. 2013. Genetic variant in APE1 gene promoter contributes to cervical cancer risk. Am J Obstet Gynecol 209:360.e1–367.e1.

Woodman CB, Collins S, Winter H, Bailey A, Ellis J, Prior P, Yates M, Rollason TP, Young LS. 2001. Natural history of cervical human papillomavirus infection in young women: A longitudinal cohort study. Lancet 357:1831–1836.

Wright TC Jr, Stoler MH, Sharma A, Zhang G, Behrens C, Wright TL, ATHENA (Addressing The Need for Advanced HPV Diagnostics) Study Group. 2011. Evaluation of HPV-16 and HPV-18 genotyping for the triage of women with high-risk HPV+ cytology-negative results. Am J Clin Pathol 136:578–586.

Zhao M, Qiu L, Tao N, Zhang L, Wu X, She Q, Zeng F, Wang Y, Wei S, Wu X. 2013. HLA DRB allele polymorphisms and risk of cervical cancer associated with human papillomavirus infection: A population study in China. Eur J Gynaecol Oncol 34:54–59.

SUPPORTING INFORMATION

Additional supporting information may be found in the online version of this article at the publisher's web-site.

JSHC
Japan Society of Histochemistry and Cytochemistry
Established 1959

Acta Histochem. Cytochem. 47 (3): 85–94, 2014
doi: 10.1267/ahc.13040

ABCC11/MRP8 Expression in the Gastrointestinal Tract and a Novel Role for Pepsinogen Secretion

Hirofumi Matsumoto[1], Tomoshi Tsuchiya[1], Koh-ichiro Yoshiura[2], Tomayoshi Hayashi[3], Shigekazu Hidaka[1], Atsushi Nanashima[1] and Takeshi Nagayasu[1]

[1]Division of Surgical Oncology, Department of Surgical Oncology, Nagasaki University Graduate School of Biomedical Sciences, [2]Department of Human Genetics, Nagasaki University Graduate School of Biomedical Sciences, 1–7–1 Sakamoto, Nagasaki 852–8501, Japan and [3]Department of Pathology, Nagasaki University Hospital, Nagasaki, Japan

Received November 14, 2013; accepted April 2, 2014; published online June 18, 2014

ATP-binding cassette (ABC) transporters are involved in chemotherapy resistance. Multidrug-resistance protein 8 (ABCC11/MRP8) is also involved in 5-fluorouracil (5-FU) metabolism. 5-FU and its derivatives are widely used in the treatment of gastrointestinal tract cancers, but little is known about the contribution of ABCC11/MRP8 to gastrointestinal tract and related cancers. Here, we report our investigation of ABCC11/MRP8 expression in normal and cancerous gastrointestinal tract tissues and reveal its novel role in the gastric mucosa. In tissue microarray and surgically resected cancer specimens, immunohistochemical (IHC) staining revealed significantly reduced expression of ABCC11/MRP8 in gastrointestinal tract cancers compared with other cancers. In contrast, strong ABCC11/MRP8 expression was observed in normal gastric mucosa. Additional immunofluorescence assays revealed co-localization of ABCC11/MRP8 and pepsinogen I in normal gastric chief cells. Quantitative PCR and Western blot analysis also revealed significant expression of ABCC11/MRP8 in fundic mucosa where the chief cells are mainly located. Furthermore, the *ABCC11* mRNA-suppressed NCI-N87 gastric cancer cell line failed to secret pepsinogen I extracellularly. Thus, low expression of ABCC11/MRP8 is consistent with chemotherapeutic regimens using 5-FU and its derivatives in gastrointestinal tract cancers. Our results indicated a novel function of ABCC11/MRP8 in the regulation of pepsinogen I secretion in the normal gastric chief cells.

Key words: ABCC11/MRP8, ABC transporter, pepsinogen I, gastric chief cells, gastrointestinal tract

I. Introduction

The ATP-binding cassette (ABC) genes represent the largest family of transmembrane proteins. These proteins bind ATP and use the energy to drive the transport of various molecules across all cell membranes [6]. Until today, 48 ABC transporters have been identified in humans [8, 22, 28]. Among those, ABC transporters, sub-family C, member 11, coding multidrug-resistance protein 8 (ABCC11/MRP8) was first cloned from a cDNA library derived from normal human breast and liver [8, 22, 28]. It contains two conserved nucleotide-binding domains and 12 putative transmembrane domains classified as "full transporters" [22].

ABC transporters confer drug resistance against a broad range of chemotherapeutic agents [8]. ABCC11/MRP8 has been shown to act as a metabolic apparatus of 5-fluorouracil (5-FU) [14], which is widely used in cancer chemotherapy [16]. 5-FU and its derivatives are metabolized to 5-fluoro-2'-deoxyuridine 5'-monophosphate (FdUMP) by intracellular metabolic enzymes [16, 24, 25].

Correspondence to: Takeshi Nagayasu, MD, PhD, Department of Surgical Oncology, Nagasaki University Graduate School of Biomedical Sciences, 1–7–1 Sakamoto, Nagasaki 852–8501, Japan.
E-mail: nagayasu@nagasaki-u.ac.jp

© 2014 The Japan Society of Histochemistry and Cytochemistry

FdUMP is actively transported by ABCC11/MRP8, which has been suggested to be involved in conferring resistance to 5-FU [4, 5, 7, 31, 36]. In gastrointestinal tract cancers, 5-FU-based drugs are ordinarily selected for first-line chemotherapy, and these drugs are known to improve both overall and disease-free survival [25, 32].

On the other hand, ABCC11/MRP8 has specific roles in secretory organs. Our previous studies demonstrated that ABCC11/MRP8 was responsible for earwax secretion [27, 35]. In summary, a SNP (538G>A, Gly180Arg) in the ABCC11 gene determines the type of earwax, and the GG homozygous and GA heterozygous genotypes correspond to wet earwax [35]. Similarly, ABCC11 wild type is responsible for the secretion of pre-odoriferous compounds from the axillary apocrine gland [27], and associated with axillary osmidrosis [11, 21, 30]. In addition, ABCC11/MRP8 plays a role in colostrum secretion by acting as an efflux pump and is a peripheral factor independent of endocrine control [20]. These findings and the reported variety of transport molecules associated with ABCC11/MRP8 suggest that it may also have some effect on other secretory organs.

ABCC11/MRP8 is expressed in normal tissues including the brain, breasts, lungs, liver, kidney, placenta, prostate, testes, and apocrine glands, as well as in cancerous tissues [3, 4, 34]. However, the contribution of ABCC11/MRP8 to gastrointestinal tract and related cancers remains poorly understood. The main purpose of this study was to clarify the expression profile of ABCC11/MRP8 and its possible function in gastrointestinal tract and related cancers.

II. Materials and Methods

Patients and tissue samples

Tissue samples were obtained with informed consent from 87 patients treated surgically at Nagasaki University Hospital (Table 1). Formalin-fixed paraffin-embedded (FFPE) sections were subjected to immunohistochemical (IHC) staining and immunofluorescence (IF) assay. Fresh frozen samples of normal gastric mucosa were also obtained from gastric cancer patients. A tissue microarray (Human Multiple Normal and Cancer Tissue Array, Protein Biotechnologies, Ramona, CA, USA) containing 48 normal tissues and 48 solid cancers was also used to analyze ABCC11/MRP8 expression.

Cell lines and related chemicals

Human gastric cancer cell line NCI-N87 (CRL 5822) was obtained from the American Type Culture Collection (ATCC, Manassas, VA, USA). Human gastric cancer cell line HGC-27 (RCB 0500), which did not have the morphological and enzyme-histochemical characteristics of glandular epithelial cells [1], was provided by RIKEN BRC through the National Bio-Resource Project of the MEXT, Japan. These cell lines were characterized and authenticated at the repository by methods such as mycoplasma infection testing and DNA identification testing (short tandem repeat analysis) and were used within 6 months of purchase. The cells were maintained in RPMI 1640 (Life Technologies, Carlsbad, CA, USA) supplemented with 10% (v/v) heat-inactivated fetal bovine serum (Life Technologies) and 1% (v/w) penicillin/streptomycin (Life Technologies). Cells were subcultured using 0.05% trypsin-0.53 mM EDTA solution (Life Technologies). For the *ABCC11* mRNA suppression assay, cells were cultured in Opti-MEM I serum-free medium (Life Technologies).

Antibodies

For IHC staining, primary antibodies were used at the following concentrations: rabbit polyclonal anti-human ABCC11/MRP8 antibody (Santa Cruz Biotechnology, Santa Cruz, CA, USA), 1:200 and mouse monoclonal anti-human pepsinogen I antibody (Sanbio BV, Uden, The Netherlands), 1:500. Horseradish peroxidase (HRP)-conjugated goat polyclonal anti-rabbit IgG (Nichirei Biosciences, Tokyo, Japan) and HRP-conjugated goat polyclonal anti-mouse IgG (Nichirei Biosciences) were used as

Table 1. *Characteristics of patients and ABCC11/MRP8 IHC staining scores*

	n (male, female)	Mean Age (range)	IHC Staining Score
Breast Cancer	14 (0, 14)	61.9 (49–88)	1.75±0.51***
HCC/CCC	10 (10, 0)	67.2 (53–76)	1.65±0.88**
Pancreatic Cancer	5 (2, 3)	67.6 (52–81)	1.00±0.35*
Lung Cancer	19 (14, 5)	65.1 (42–79)	1.05±0.69**
Thyroid Cancer	5 (2, 3)	51.4 (24–76)	0.80±0.76
Gastrointestinal tract Cancer	34 (17, 17)	64.1 (43–88)	0.44±0.54
Esophageal	5 (3, 2)	65.4 (63–69)	0.70±0.57
Gastric	16 (6, 10)	61.7 (37–79)	0.25±0.45
Colorectal	13 (8, 5)	66.7 (43–82)	0.54±0.59
Total	87 (45, 42)	63.8 (24–88)	1.00±0.80

n, number of patients analyzed; HCC, hepatocellular carcinoma; CCC, cholangiocellular carcinoma. IHC Staining score was calculated by two investigators using clarification criteria as described. Data represent mean values±SD. */ **/ ***; significant difference between gastrointestinal tract cancer and cancers of other organs, $P<0.05$ (*), $P<0.01$ (**), and $P<0.001$ (***), based on a nonparametric Mann–Whitney *U* test.

detecting antibodies. Alexa Fluor 488-conjugated goat polyclonal anti-rabbit IgG (Life Technologies), 1:2000 and Alexa Fluor 594-conjugated goat polyclonal anti-mouse IgG (Life Technologies), 1:2000 were also used as detecting antibodies in the IF assay. In the Western blot analysis, additional mouse monoclonal anti-actin antibody (Abcam, Cambridge, MA, USA) or anti-GAPDH antibody were used as internal controls.

Immunohistochemical staining and immunofluorescence assay

FFPE sections were deparaffinized in dimethylbenzene and rehydrated through a graded alcohol series. After antigen retrieval in HistoVT One (Nacalai Tesque, Kyoto, Japan) (95°C, 20 min), blocking of endogenous peroxidase activity in 3% H_2O_2 solution, sections were incubated with each primary antibody (4°C, overnight). After washing in PBS, sections were incubated with the detecting antibody (room temperature, one hour). For IHC staining, sections were visualized with 3,3'-diaminobenzidine tetra hydrochloride (DAB: brown) or 3-amino-9-ethylcarbazole (AEC: red) and counterstained with hematoxylin. The sections visualized with DAB were dehydrated with alcohol and dimethylbenzene and mounted in a conventional fashion. Sections visualized with AEC were mounted in aqueous media without dehydration. Normal breast tissue specimens, which moderately expressed ABCC11/MRP8 [4] were prepared as positive controls in all cases. Negative controls were also prepared in all cases by substituting the primary antibody. The IHC staining scores were calculated by two investigators using the following criteria: score 0, no expression; score 1, low expression <10%; score 2, moderate expression >10% or diffuse staining; score 3, strong expression >90%, or strong focal staining. The mean values were determined for each cancer.

For IF assay, sections were mounted in mounting media with 4',6-diamidino-2-phenylindole (DAPI). Double IF assays were observed by confocal laser scanning microscopy (LSM 510 META, Carl Zeiss, Oberkochen, Germany) or fluorescence microscopy (BX70, Olympus, Tokyo, Japan).

ELISA

The amount of pepsinogen I secreted in culture medium was measured by specific ELISA tests (Biohit Plc, Helsinki, Finland). All experiments were performed in duplicate. The mean values of each sample were normalized by the concentration of the total protein.

Western blot analysis

To extract whole proteins, the gastric mucosa specimens were homogenized in radio-immunoprecipitation assay (RIPA) buffer (Nacalai Tesque) using a Bioruptor (Tosho Denki, Yokohama, Japan). Following centrifugation at 5,000 g for 10 min, the supernatant fraction was collected. For culture samples, the supernatant fraction of each culture medium was collected. Whole cell lysates were prepared as cytoplasmic fractions using RIPA buffer (Nacalai Tesque). The protein concentrations of all samples were quantified using a BCA Protein Assay Kit (Thermo Fisher Scientific, Waltham, MA, USA). The same amount of protein from each sample was prepared in a sample buffer (ATTO, Tokyo, Japan) containing SDS. The proteins were then separated by 8% SDS-PAGE (Tefco, Tokyo, Japan) and electro-transferred to polyvinylidene difluoride (PVDF) membranes (GE Healthcare, Buckinghamshire, UK). One hour after blocking in Tris-buffered saline containing 0.1% (v/v) Tween 20 (TBS-T) and 1% (w/v) skim milk, primary and detecting antibodies were used at their own concentrations. HRP-dependent luminescence was developed using ECL Plus Western Blotting Detecting Reagents (GE Healthcare), and was detected with a Lumino Imaging Analyzer FluorChem Imaging System (Cell Biosciences, Santa Clara, CA, USA) according to the manufacturer's specifications.

Total RNA extraction and quantitative PCR

Total RNA was extracted using High Pure RNA Isolation Kit (Roche Diagnostics, Mannheim, Germany). Reverse transcription was performed with 2 μg of the total RNA using High-Capacity Reverse Transcription (Life Technologies). Quantitative PCR analysis was performed using a Life Technologies Prism 7900HT Sequence Detection System. TaqMan probes and primers for ABCC11/MRP8 were obtained as assay-on-demand gene expression products (assay ID: Hs01090768_m1, Life Technologies). The mRNA of pepsinogen I was analyzed using the following primer set (sense primer, 5'-CCC GTC TTT GAC AAC ATC TG-3'; anti-sense primer, 5'-CGC TGC CAC TCT TGT CAT C-3'). The mRNA of GAPDH was used as an endogenous control (assay ID: Hs99999905_m1, Life Technologies). The thermal cycler conditions were as follows: held for 10 min at 95°C followed by two-step PCR for 45 cycles of 95°C for 15 sec and 60°C for 1 min. All experiments were performed in quadruplicate. The number of transcripts was calculated from a standard curve obtained by plotting the known input of six different concentrations versus the PCR cycle number at which the detected fluorescence intensity reached a fixed value. Amplification data were analyzed with Prism Sequence Detection Software version 2.1 (Life Technologies). For each sample, data were normalized to *GAPDH*.

ABCC11 mRNA suppression by RNA interference

Cells were suspended in serum-free Opti-MEM I medium (Life Technologies) at a concentration of 10^5 cells/well. Small interfering RNA (siRNA) for *ABCC11* (predesigned siRNA, ID: s39907) and negative-control siRNA (Silencer negative control siRNA, ID: AM4611) were purchased from Life Technologies. Prepared cells were transfected with siRNA according to the manufacturer's specifications using 5 μl siPORT NeoFX Transfection

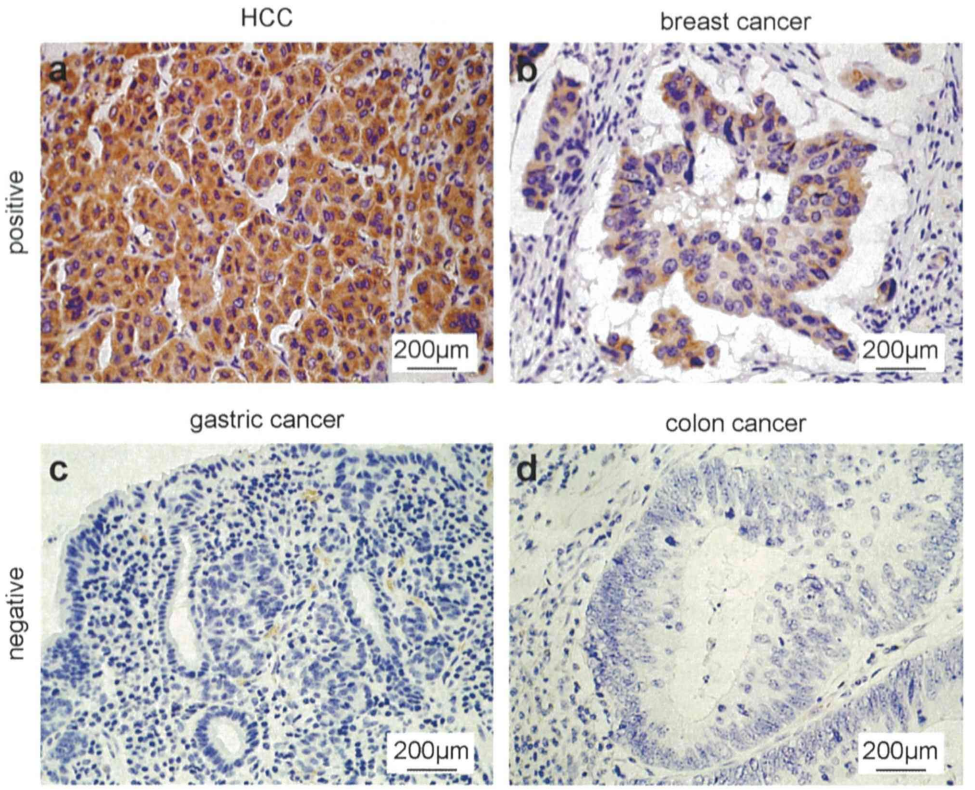

Fig. 1. Representative positive- and negative-stained cancer specimens obtained from cancer patients. **a**, HCC (moderately differentiated); **b**, breast cancer (invasive ductal carcinoma); **c**, gastric cancer (moderately differentiated adenocarcinoma); **d**, colon cancer (well differentiated adenocarcinoma). Upper specimens are ABCC11/MRP8 positive and lower specimens are negative.

agent (Life Technologies) to produce a final RNA concentration of 50 nmol/l in serum-free medium. The cells were harvested after two days of transfection. The efficiency of siRNA transfection was determined by quantitative PCR, and WST-8 [2-(2-methoxy-4-nitrophenyl)-3-(4-nitrophenyl)-5-(2,4-disulfophenyl)-2H-tetrazolium monosodium salt] [12] (Nacalai Tesque) assay was also performed to determine cell viability.

Statistical analysis

Statistical significance was assessed using either unpaired Student's *t*-test for parametric data or Mann–Whitney *U* test for nonparametric data. StatView software version 5.0 (SAS Institute, Cary, NC, USA) was used for all statistical analyses.

III. Results

ABCC11/MRP8 expression in solid cancers

Representative positive- and negative-stained cancer specimens obtained from cancer patients are shown in Figure 1. Genetically, the expression of ABCC11/MRP8 was proved in normal tissues of liver and breast by PCR [3, 34]. In our experiments, almost all specimens of HCC and breast cancer were ABCC11/MRP8 positive, and they were observed in the cytoplasm (Fig. 1a and b). In contrast, almost all specimens of gastric cancer and colon cancer were negative (Fig. 1c and d).

Representative positive- and negative-stained cancer specimens in the tissue microarray (48 normal tissues and 48 cancers) are shown in Figure 2A. ABCC11/MRP8 expression in 87 cancer patients was analyzed using the IHC Staining Score based on the classification criteria. In gastrointestinal tract cancers, ABCC11/MRP8 expression was significantly lower than that in breast, HCC/CCC, pancreatic, and lung cancers (Fig. 2B).

Localization of ABCC11/MRP8 in normal stomach

ABCC11/MRP8 expression was observed in the normal gastric mucosa. In low magnification images, ABCC11/MRP8 immunopositive cells are gathered in the fundic glands similarly to pepsinogen I (Fig. 3A). In high magnification images, positive cells contained vacuolar structures in the cytoplasm, and the nuclei were pushed aside, suggesting that these were gastric chief cells (Fig. 3B). In contrast, larger, round gastric parietal cells were not stained with ABCC11/MRP8 and pepsinogen I.

To clarify the co-localization of ABCC11/MRP8 with pepsinogen I, double immunofluorescent (IF) assay was performed. In double IF assay of the normal gastric mucosa, ABCC11/MRP8-and pepsinogen I-expressing cells were completely matched (Fig. 4A and B). Pepsin-

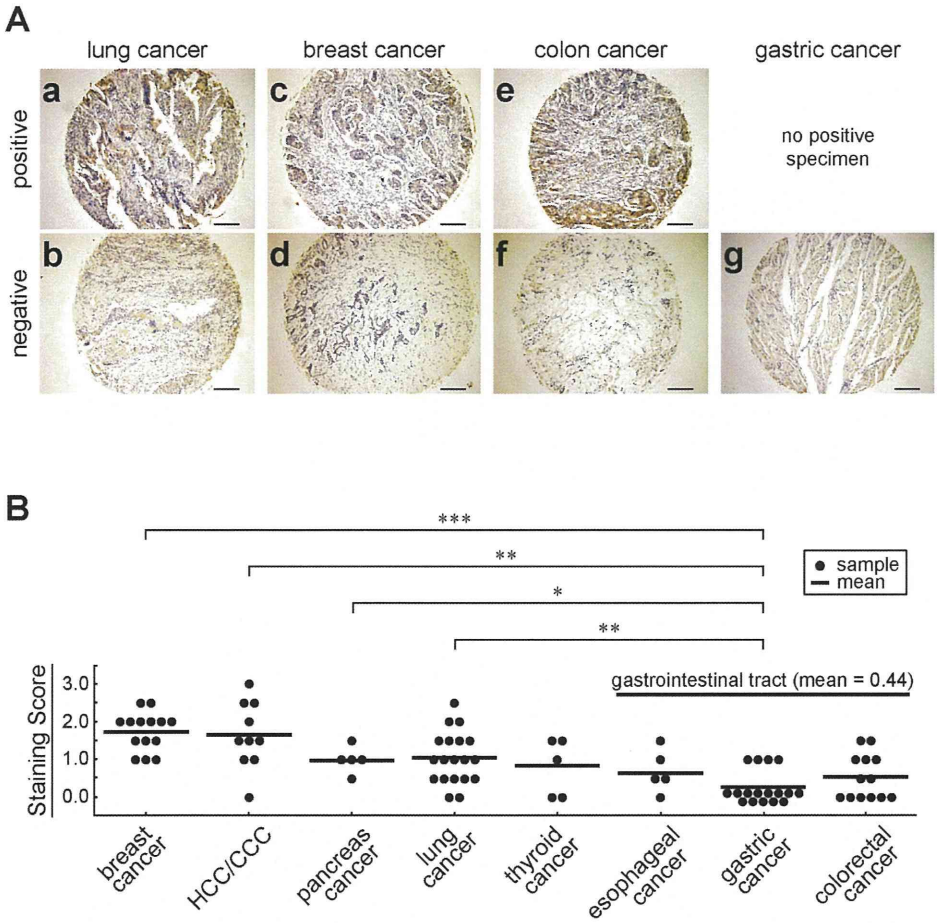

Fig. 2. **A:** Representative ABCC11/MRP8 staining of the tissue microarray. **a** and **b**, lung cancer (adenocarcinoma); **c** and **d**, breast cancer (infiltrating ductal carcinoma); **e** and **f**, colon cancer (mucinous adenocarcinoma); **g**, gastric cancer (mucinous adenocarcinoma). Upper specimens are ABCC11/MRP8 positive and lower specimens are ABCC11/MRP8 negative. Note that all gastric cancers are ABCC11/MRP8 negative. Bar=200 μm. **B:** ABCC11/MRP8 IHC Staining Scores for 87 surgically resected sections. HCC, hepatocellular carcinoma; and CCC, cholangiocellular carcinoma. Dot plots are representative of each IHC Staining Score, and horizontal bars represent the mean values. Statistical significance between cancer types was determined by a nonparametric Mann–Whitney *U* test. *, $P<0.05$; **, $P<0.01$; and ***, $P<0.001$.

producing NCI-N87 cells [2, 20] were also immunopositive for ABCC11/MRP8 and pepsinogen I, co-localizing in the cytoplasm (Fig. 4C).

Quantitative PCR assay revealed significant expression of ABCC11/MRP8 in gastric fundic mucosa ($P<0.005$), which overlapped the distribution of gastric fundic glands (Fig. 5A). Western blot analysis of ABCC11/MRP8 also showed limited localization in fundic mucosa (Fig. 5B).

Alteration of pepsinogen I secretion by ABCC11 siRNA transfection

NCI-N87 cells secret pepsin and they have been used as a model of human gastric epithelial functions [2, 20]. To investigate the contribution of pepsinogen I secretion by *ABCC11* mRNA expression, NCI-N87 cells were used in an *ABCC11* mRNA suppression assay with siRNA. Figure 6A shows almost 80% reduction in *ABCC11* expression in NCI-N87 cells transfected with ABCC11 siRNA compared with control cells. ELISA assay showed that the *ABCC11* reduced by siRNA almost abolished pepsinogen I secretion to the extracellular culture medium without decreasing cell viability ($P<0.005$ vs. negative siRNA) (Fig. 6B and C). Although the cells transfected with ABCC11 siRNA failed to secrete pepsinogen I extracellularly, cytoplasmic *pepsinogen I* mRNA and pepsinogen I were not altered (Fig. 6D and E).

IV. Discussion

In the present study, we investigated the expression of ABCC11/MRP8 in various cancers and revealed that this expression was reduced in gastrointestinal tract cancers compared with breast, HCC/CCC, pancreatic, and lung cancers. ABCC11/MRP8 has been reported to contribute to multidrug-resistance especially 5-FU and its derivatives [24, 31, 36]. Our finding of reduced ABCC11/MRP8 expression in gastrointestinal tract cancers supports the view

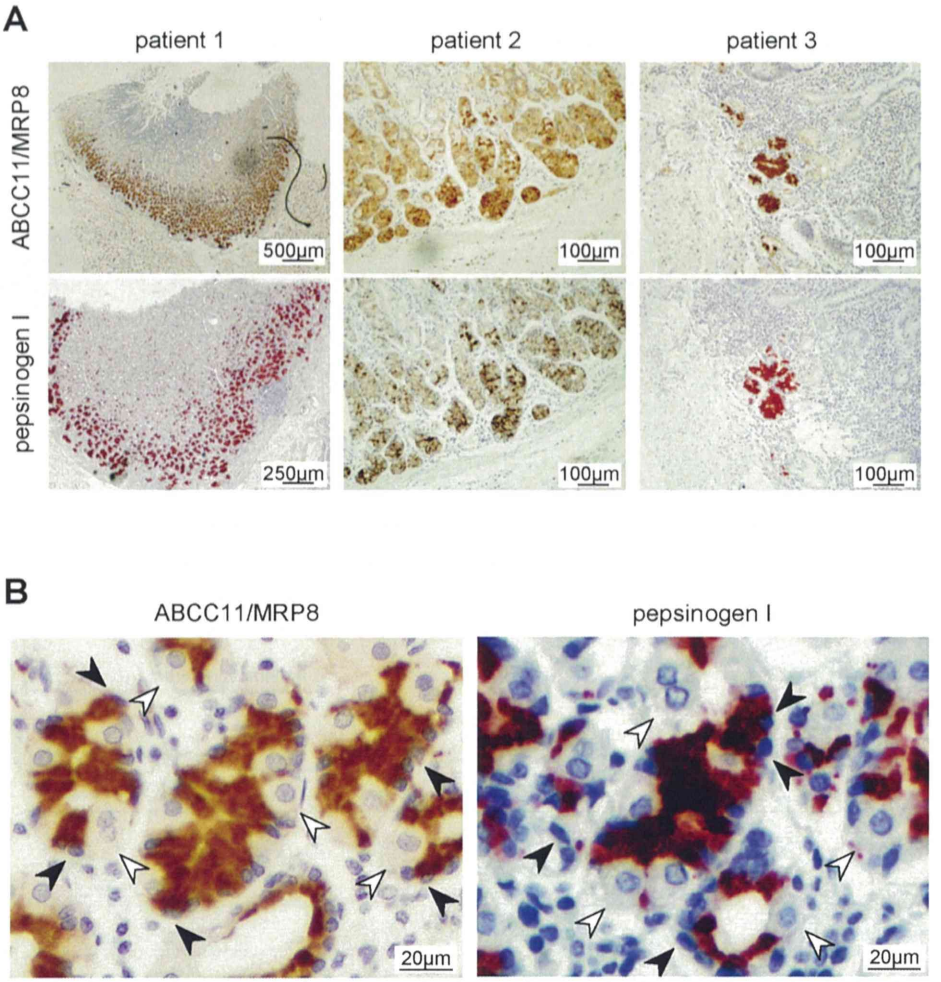

Fig. 3. **A:** Representative ABCC11/MRP8 and pepsinogen I staining images in serial sections of normal gastric mucosa obtained from three different patients. **B:** ABCC11/MRP8 and pepsinogen I staining in serial sections of surgically resected normal gastric mucosa at high magnification. Black arrowheads indicate gastric chief cells, and white arrowheads indicate gastric parietal cells.

that these cancers are sensitive to 5-FU and its derivatives, and this is consistent with findings from routine chemotherapy regimens [16]. The investigation of expression level of ABCC11/MRP8 may provide us with useful information for making choices when tailor-making chemotherapies as well as for evaluating histoculture drug response assay or collagen gel droplet embedded culture drug sensitivity test. Hlavata and colleagues analyzed the relations between transcript levels of all known ABC transporters in colorectal cancers and chemotherapy efficiency, and revealed that ABCC11/MRP8 might be a promising candidate marker for 5-FU therapy [10]. Furthermore, Uemura and colleagues demonstrated that ABCC11/MRP8 directly confers resistance to pemetrexed, a new-generation antifolate antimetabolite [31]. In gastrointestinal tract cancers, chemotherapies with pemetrexed are currently under investigation. Our findings might add further insight on the potential clinical benefits of pemetrexed in gastrointestinal tract cancers.

In the present study, the over-expressions of ABCC11/MRP8 were not observed in 16 gastric cancer patients. However, reported cell line based studies have demonstrated that increased expression of ABCC11/MRP8 directly conferred chemoresistance [24, 31]. Considering the colorectal cancer studies, the relations between the expression levels of ABCC11/MRP8 and chemoresistance to 5-FU might be observed also in gastric cancers. Additional investigations are required to elucidate the possible role of biological effect of ABCC11/MRP8 for chemoresistance in gastric cancers.

We also intensively analyzed ABCC11/MRP8 expression in normal gastric mucosa because of the strong immunohistochemical staining in gastric chief cells. To the best of our knowledge, the present study is the first to reveal the expression of ABCC11/MRP8 in normal gastric mucosa. Interestingly, ABCC11/MRP8 expression was observed in normal gastric mucosa. However, it was almost negative in gastric cancers regardless of their histological types or dif-

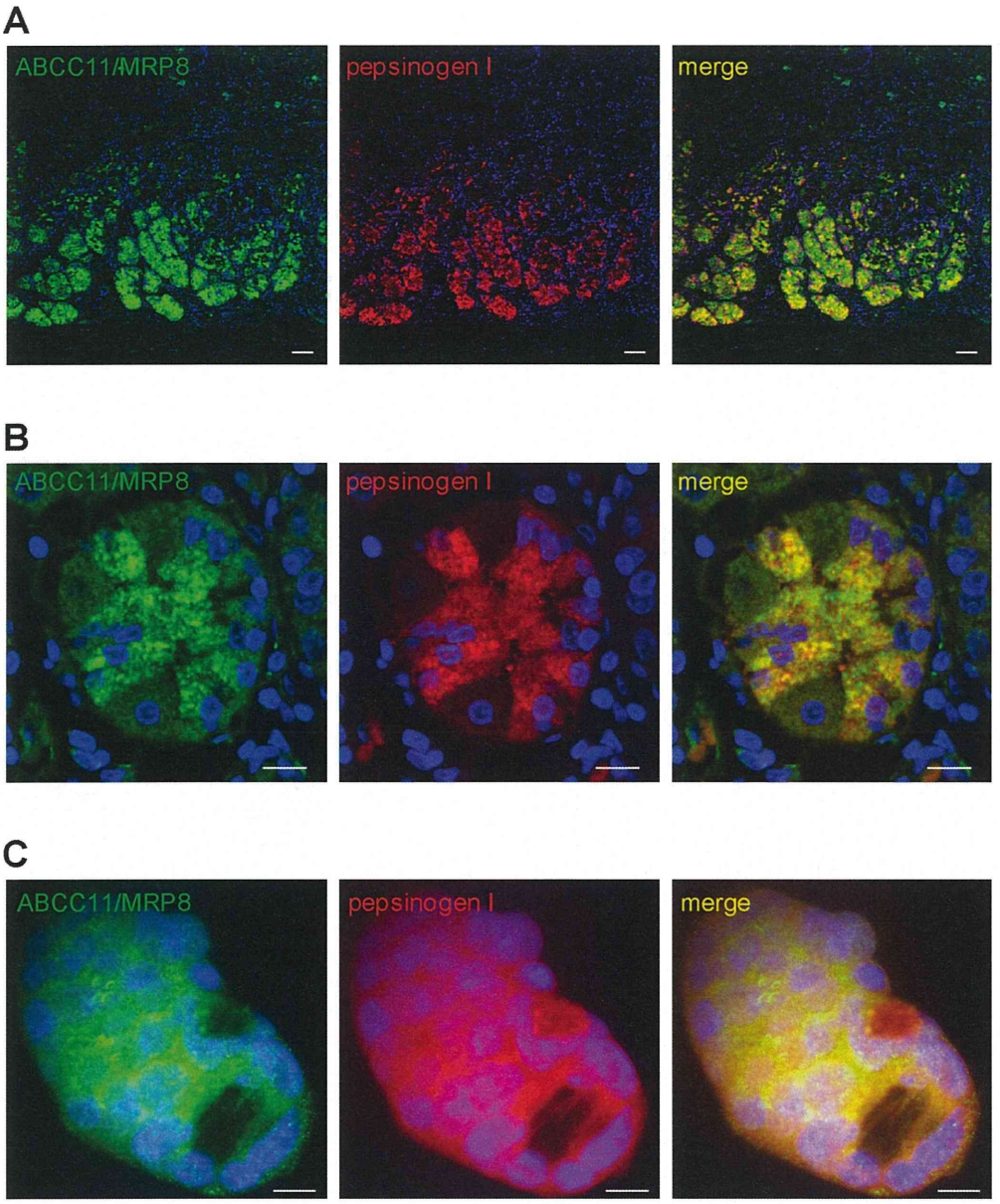

Fig. 4. Double immunofluorescence assay of surgically resected normal gastric mucosa and NCI-N87 cells with the following fluorescence-labeled antibodies: green, ABCC11/MRP8; red, pepsinogen I; and blue, DAPI. **A:** Low magnification of normal gastric mucosa, confocal laser scanning microscopy. Bar=50 μm. **B:** High magnification of normal gastric mucosa, confocal laser scanning microscopy. Bar=10 μm. **C:** High magnification of NCI-N87 cells fixed with 3.7% paraformaldehyde, fluorescence microscopy. Bar=10 μm.

ferentiations (poorly adenocarcinoma; 6, signet ring cell carcinoma; 5, moderately adenocarcinoma; 3, others; 3). This discrepancy may be explained by the origin of gastric cancers. In humans, intestinal metaplasia and spasmolytic polypeptide-expressing metaplasia (SPEM) are associated with the precancerous stomach [33]. Nozaki and colleagues reported that gastric chief cells transdifferentiated into SPEM cells with down-regulated mature chief cell markers including pepsinogen I [23].

Pepsinogen I is secreted by gastric chief cells in fundic glands around the upper stomach. Pepsinogen II is secreted in the pyloric and Brunner's glands around the lower stomach as well as fundic gland [9, 13]. The present study indicated that ABCC11/MRP8 was expressed in the upper portion of the gastric mucosa. Therefore, we hypothesized that ABCC11/MRP8 regulated pepsinogen I secretion, and not pepsinogen II. Pepsinogen synthesis and secretion are regulated by positive and negative feedback mechanisms [26]. In theory, pepsinogens are synthesized on the endoplasmic reticulum and modified at the Golgi body, then, once stored in granules, they are secreted through an exocytosis process [9, 26]. The releasing process and modu-